[American Journal of Science, Vol. 305, November, 2005, P. 875–918]

American Journal of Science

NOVEMBER 2005

COASTAL OCEAN AND CARBONATE SYSTEMS IN THE HIGH CO_2 WORLD OF THE ANTHROPOCENE

ANDREAS J. ANDERSSON*†, FRED T. MACKENZIE*, and ABRAHAM LERMAN**

ABSTRACT. The behavior of the ocean carbon cycle has been, and will continue to be, modified by the increase in atmospheric CO_2 due to fossil fuel combustion and land-use emissions of this gas. The consequences of a high-CO_2 world and increasing riverine transport of organic matter and nutrients arising from human activities were investigated by means of two biogeochemical box models. Model numerical simulations ranging from the year 1700 to 2300 show that the global coastal ocean changes from a net source to a net sink of atmospheric CO_2 over time; in the 18th and 19th centuries, the direction of the CO_2 flux was from coastal surface waters to the atmosphere, whereas at present or in the near future the net CO_2 flux is into coastal surface waters. These results agree well with recent syntheses of measurements of air-sea CO_2 exchange fluxes from various coastal ocean environments. The model calculations also show that coastal ocean surface water carbonate saturation state would decrease 46 percent by the year 2100 and 73 percent by 2300. Observational evidence from the Pacific and Atlantic Oceans shows that the carbonate saturation state of surface ocean waters has already declined during recent decades. For atolls and other semi-enclosed carbonate systems, the rate of decline depends strongly on the residence time of the water in the system. Based on the experimentally observed positive relationship between saturation state and calcification rate for many calcifying organisms, biogenic production of $CaCO_3$ may decrease by 42 percent by the year 2100 and by 85 to 90 percent by 2300 relative to its value of about 24×10^{12} moles C/yr in the year 2000. If the predicted change in carbonate production were to occur along with rising temperatures, it would make it difficult for coral reef and other carbonate systems, to exist as we know them now into future centuries. Because high-latitude, cold-water carbonates presently occur in waters closer to saturation with respect to carbonate minerals than the more strongly supersaturated waters of the lower latitudes, it might be anticipated that the cool-water carbonate systems might feel the effects of rising atmospheric CO_2 (and temperature) before those at lower latitudes. In addition, modeling results show that the carbonate saturation state of coastal sediment pore water will decrease in the future owing to a decreasing pore water pH and increasing CO_2 concentrations attributable to greater deposition and remineralization of land-derived and *in situ* produced organic matter in sediments. The lowered carbonate saturation state drives selective dissolution of metastable carbonate minerals while a metastable equilibrium is maintained between the pore water and the most soluble carbonate phase present in the sediments. In the future, the average composition of carbonate sediments and cements may change as the more soluble Mg-calcites and aragonite are preferentially dissolved and phases of lower solubility, such as calcites with lower magnesium content, increase in percentage abundance in the sediments.

*Department of Oceanography, School of Ocean and Earth Science and Technology, University of Hawaii, 1000 Pope Road, Honolulu, Hawaii 96822

**Department of Geological Sciences, Northwestern University, 1850 Campus Drive, Evanston, Illinois 60208-2150

†Corresponding author: Andreas J. Andersson, aj@soest.hawaii.edu

INTRODUCTION

In recent years there has been considerable discussion concerning the effects of rising atmospheric CO_2 and temperature on coral reef ecosystems (see for example, Gattuso and others, 1999; Kleypas and others, 1999, 2001; Langdon and others, 2000, 2003; Andersson and others, 2003; Buddemeier and others, 2004; McNeil and others, 2004). Continuous burning of fossil fuels will lead to continuous future increases in atmospheric CO_2 and dissolved inorganic carbon in the atmospheric and oceanic sinks of anthropogenic carbon, respectively. Future global mean temperature is also likely to increase, although the estimated magnitude of the increase varies depending on the future emission scenarios of greenhouse and sulfur gases into the atmosphere, the changing strengths of the land and ocean sinks of CO_2, and other factors. As the oceans have absorbed CO_2, their saturation state with respect to carbonate minerals has fallen and will continue to fall in the future (Kleypas and others, 1999; Andersson and others, 2003; McNeil and others, 2004; Feely and others, 2004). This decrease in carbonate saturation state has led several investigators, among those cited above, to infer that carbonate secreting organisms may have difficulty in maintaining calcification at present rates and that coral reef ecosystems may be subject to enhanced biological and mechanical erosion in the future. Most of these inferences have been drawn based on experimental and a few field observations. In this paper we use two established models, *TOTEM* (Terrestrial Ocean aTmosphere Ecosystem Model) (Ver and others, 1994, 1998, 1999a, 1999b; Ver, ms, 1998; Mackenzie and others, 1998, 2000, 2002) and *SOCM* (Shallow–water Ocean Carbonate Model) (Andersson, ms, 2003; Andersson and others, 2003; Andersson and Mackenzie, 2004; Mackenzie and others, 2004a, 2004b) to investigate the relationships between saturation state and calcification rate, as well as the overall behavior of the CO_2-carbonic acid–carbonate sediment system in the shallow-water ocean throughout the past 300 years of Earth's history and into the future to the year 2300.

TOTEM (as referenced above) is a process-driven biogeochemical box model that takes into account physical mixing in the ocean and represents the global atmospheric, terrestrial, and coastal and pelagic oceanic domains. *TOTEM* is comprised of thirteen reservoirs: the atmosphere; six terrestrial reservoirs (living biota, humus, inorganic soil, continental soilwater, shallow groundwater, and lakes); three coastal–zone reservoirs (organic matter, surface water, and sediments); and three open ocean reservoirs (organic matter, surface water, and deep water). The model is based on parameterization of physical, biogeochemical, and ecological processes affecting the global environmental system. Two of the major characteristics of *TOTEM* are that it couples the biogeochemical cycles of C, N, P, and S through processes such as organic productivity and it links the land phytomass and continental soils with the coastal ocean reservoir, which interacts with the open ocean through surface water exchange and upwelling. The model was employed in this study to generate data that were used as inputs to *SOCM* that is described in the following section (MODEL METHODOLOGY section). In the BIOGEOCHEMICAL CONSEQUENCES OF INCREASING ATMOSPHERIC CO_2 section, the consequences of increasing atmospheric CO_2 and temperature for the global coastal ocean are discussed from a biological, chemical, and geological perspective, presenting the model results of *SOCM* until the year 2100 in conjunction with basic background information, theory, and observational data. Beyond the year 2100, the model simulations become increasingly speculative, partly because the major forcings on the system and their future changes over time are less well known. Hence these results are presented separately in the THE CENTURY-SCALE FUTURE OF THE COASTAL CARBONATE SYSTEM section, followed by a general discussion on the full 600 years of model simulations (DISCUSSION OF 600 YEARS OF THE

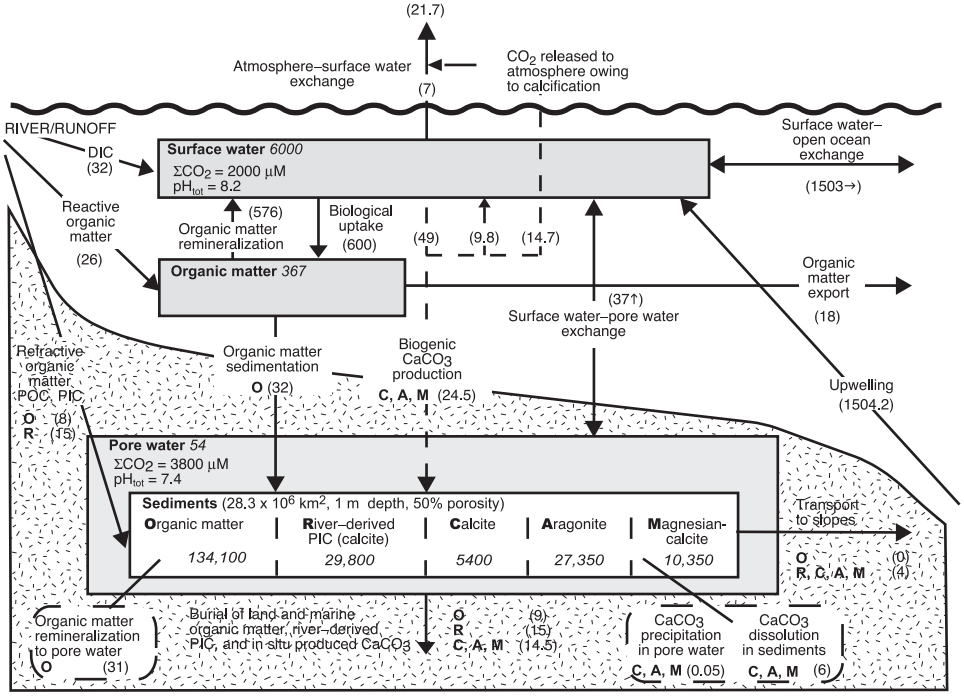

Fig. 1. Schematic of the Shallow–water Ocean Carbonate Model (*SOCM*) and pre–industrial carbon estimates adopted in the current simulations (Andersson, ms, 2003). *SOCM* consists of two major domains representing the water column (surface water and organic matter) and the pore water–sediment system (pore water, sediment organic matter, river–derived particulate inorganic carbon (PIC), calcite, aragonite, and 15 mol % magnesian calcite). Reservoir masses (shown in italics) are in 10^{12} mol C. Arrows denote carbon fluxes between reservoirs in 10^{12} mol C yr^{-1} (shown inside parentheses). For two–way arrows the direction of the net flux is shown next to the flux estimate. The dashed lines indicate carbon flux owing to $CaCO_3$ production (eq 16). 2 mol of C are removed from the water column for every mol of $CaCO_3$ precipitated, 1 mol of C is released back to the water column as CO_2 from which 0.4 mol C remains in the surface water reservoir and 0.6 mol C evades to the atmosphere.

CO_2–CARBONATE SYSTEM section). Finally, we discuss briefly some aspects of the ocean carbon cycle beyond the year 2300 (BEYOND THE YEAR 2300 section).

MODEL METHODOLOGY

The Shallow–water Ocean Carbonate Model (*SOCM)* is a process–driven biogeochemical box model representative of the global shallow-water ocean environment including coastal zones, reefs, banks and continental shelves (28.3×10^6 km^2) (Milliman, 1974). Details and some of the earlier results of the model are given in Andersson (ms, 2003), Andersson and others (2003), Andersson and Mackenzie (2004) and Mackenzie and others (2004a, 2004b). The *SOCM* consists of two different major domains, a surface water domain and a pore water–sediment domain (fig. 1). The surface water domain contains the reservoirs of dissolved inorganic carbon (DIC) and organic matter [dissolved organic carbon (DOC), organic detritus and living biota]. The pore water–sediment domain contains the reservoirs of organic matter, refractive particulate inorganic carbon (originating from continental erosion), *in situ* produced calcite, aragonite, 15 mol percent magnesian calcite representative of magnesian calcite compositions, and a pore water reservoir of average composition based on data from the Bahamas and elsewhere (Thorstenson and Mackenzie, 1974;

Morse and others, 1985; Morse and Mackenzie, 1990). Differential equations are expressed in the general form (table 1, where fluxes F are denoted CF):

$$\frac{dC_i}{dt} = \sum_j F_{ji} - \sum_j F_{ij} \tag{1}$$

where C is the mass of carbon in reservoir i, F_{ij} is the flux of carbon from reservoir i to reservoir j, and F_{ji} is the flux of carbon from reservoir j to reservoir i. The fluxes include the physical transport as well as chemical production or consumption terms. The most commonly adopted flux between reservoirs is described by equations of first order kinetics:

$$F_{ij} = k_{ij}C_i \tag{2}$$

where F_{ij} is the flux of carbon from reservoir i to reservoir j, which is linearly dependent on the mass of carbon in reservoir C_i, and k_{ij} is the rate constant. In the present model, k_{ij} was defined based on the initial reservoir mass and the initial flux adopted at the initial quasi–steady state in the year 1700 (fig. 1), that is:

$$k_{ij} = \left.\frac{C_i}{F_{ij}}\right|_{t=0} \tag{3}$$

Essential Mathematical Relationships of the Model

The standard model of *SOCM* calculates the air-sea CO_2 exchange and changes in the chemical and mineralogical state of the water-sediment system that are driven by biogenic calcification, inorganic precipitation and dissolution of carbonate phases, and the production, import, and remineralization of organic matter. The mathematical relationships behind these processes are described in the next three sections.

Biogenic calcification.—Biogenic calcification is related to the concentration of total dissolved inorganic carbon (DIC) in surface water, carbonate saturation state, and sea surface temperature. The dependence of marine primary production on DIC content can be viewed as a first order relationship assuming that marine primary production is directly related to this parameter (Riebesell and others, 1993; Raven, 1993, 1997). Although this assumption is contentious, the overall increase in DIC relative to its initial concentration due to increased atmospheric CO_2 is small and has only a minor effect on the rate of calcification in the current model simulations; hence, the first-order relationship provides a conservative estimate of the effect of decreasing carbonate saturation state on the rate of calcification. In model simulations, dependence of biogenic calcification on carbonate saturation state was expressed in a first case as a linear relationship derived from multiple experiments on corals and coralline algae (Gattuso and others, 1999):

$$R_\Omega = 21.3\Omega + 12, \tag{4}$$

and in a second case by a curvilinear relationship based on the experimental results for the coral *Stylophora pistillata* (Gattuso and others, 1998; Leclerq and others, 2002):

$$R_\Omega = 228(1 - e^{-\Omega/0.69}) - 128, \tag{5}$$

where R_Ω is the relative rate of calcification (approximately equal to 100 at the initial conditions) and Ω is the surface seawater saturation state with respect to aragonite. Ω is defined in equation (24). It should be pointed out that the relationship derived for *Stylophora pistillata* may not be fully representative of the response of this species to increasing CO_2 and subsequent changes in seawater carbonate chemistry because the saturation state (Ω) was manipulated by altering the calcium concentration rather

TABLE 1

SOCM mass balance and flux equations. Reservoirs are annotated C_i, where C_i refers to the total mass of carbon in reservoir i. Fluxes are annotated CF_{ij}, where CF_{ij} refers to the flux of carbon between reservoirs i and j. Rate constants are annotated kC_{ij}. A two-way arrow ($\updownarrow$) indicates that the flux can be either positive or negative.

Reservoir	Annotation	Mass balance equations
1. Surface water	C_1	$dC_1(t)/dt = CF_{R1}(t) + CF_{A1}(t) + CF_{O1}(t) + CF_{Ou1}(t) + CF_{31}(t) + CF_{21}(t) - CF_{1A}(t) - CF_{1O}(t) - CF_{13}(t) - CF_{12}(t) - CF_{16}(t) - CF_{17}(t) - CF_{18}(t)$
2. Surface water organic matter	C_2	$dC_2(t)/dt = CF_{R2}(t) + CF_{12}(t) - CF_{21}(t) - CF_{2O}(t) - CF_{24}(t)$
3. Pore water	C_3	$dC_3(t)/dt = CF_{13}(t) + CF_{43}(t) + CF_{53}(t) + CF_{63}(t) + CF_{73}(t) + CF_{83}(t) - CF_{31}(t) - CF_{35}(t) - CF_{36}(t) - CF_{37}(t) - CF_{38}(t)$
4. Sediment organic matter	C_4	$dC_4(t)/dt = CF_{R4}(t) + CF_{24}(t) - CF_{43}(t) - CF_{4B}(t) - CF_{4O}(t)$
5. Sediment river derived PIC	C_5	$dC_5(t)/dt = CF_{R5}(t) - CF_{53}(t) - CF_{5B}(t) - CF_{5O}(t)$
6. Sediment calcite	C_6	$dC_6(t)/dt = CF_{16}(t) + CF_{36}(t) - CF_{63}(t) - CF_{6B}(t) - CF_{6O}(t)$
7. Sediment aragonite	C_7	$dC_7(t)/dt = CF_{17}(t) + CF_{37}(t) - CF_{73}(t) - CF_{7B}(t) - CF_{7O}(t)$
8. Sediment magnesian calcite	C_8	$dC_8(t)/dt = CF_{18}(t) + CF_{38}(t) - CF_{83}(t) - CF_{8B}(t) - CF_{8O}(t)$
Atmosphere	A	
Sediment permanent burial	B	
Open ocean	O	
Open ocean, upwelling	Ou	
Rivers	R	

Flux equations: simple first order	Flux equations: special cases (see text)
$CF_{13}(t) = kC_{13} \times C_1(t)$	$CF_{12}(t) = CF_{12,\,t=0} \times [N_{1,\,t}/\,N_{1,\,t=0}] \times [P_{1,\,t}/\,P_{1,\,t=0}]$; N = nitrogen mass; P = phosphorus mass
$CF_{1\updownarrow O}(t) = kC_{1\updownarrow O} \times C_1(t)$	$CF_{16}(t) = [kC_{16} \times C_1(t)] \times [R(\Omega_{\text{Aragonite, t}})/R(\Omega_{\text{Aragonite, t=0}})] \times [R(T_t)/R(T_{t=0})]$
$CF_{21}(t) = kC_{21} \times C_2(t)$	
$CF_{24}(t) = kC_{24} \times C_2(t)$	$CF_{17}(t) = [kC_{17} \times C_1(t)] \times [R(\Omega_{\text{Calcite, t}})/R(\Omega_{\text{Calcite, t=0}})] \times [R(T_t)/R(T_{t=0})]$
$CF_{2O}(t) = kC_{2O} \times C_2(t)$	
$CF_{31}(t) = kC_{31} \times C_3(t)$	$CF_{18}(t) = [kC_{18} \times C_1(t)] \times [R(\Omega_{\text{Mg-calcite, t}})/R(\Omega_{\text{Mg-calcite, t=0}})] \times [R(T_t)/R(T_{t=0})]$
$CF_{43}(t) = kC_{43} \times C_4(t)$	
$CF_{4B}(t) = kC_{4B} \times C_4(t)$	$CF_{1\updownarrow A}(t)$, see equation (18) in the text.
$CF_{4O}(t) = 0$	
$CF_{53}(t) = kC_{53} \times C_5(t)$	$CF_{6\updownarrow 3}(t) = kC_{6\updownarrow 3} \times C_6(t) + \Delta PD(\Omega_{\text{Calcite}})$
$CF_{5B}(t) = kC_{5B} \times C_5(t)$	$CF_{7\updownarrow 3}(t) = kC_{7\updownarrow 3} \times C_7(t) + \Delta PD(\Omega_{\text{Aragonite}})$
$CF_{5O}(t) = 0$	$CF_{8\updownarrow 3}(t) = kC_{8\updownarrow 3} \times C_8(t) + \Delta PD(\Omega_{\text{Mg-calcite}})$
$CF_{6B}(t) = kC_{6B} \times C_6(t)$	$\Delta PD(\Omega_X) = PD_{x,t}(\Omega_X) - PD_{x,t=0}(\Omega_X)$
$CF_{6O}(t) = kC_{6O} \times C_6(t)$	$PD_x(\Omega_X) = D_x(\Omega_X) - P_x(\Omega_X)$
$CF_{7B}(t) = kC_{7B} \times C_7(t)$	For $\Omega_X > 1$,
$CF_{7O}(t) = kC_{7O} \times C_7(t)$	$D_x(\Omega_X) = 0$
$CF_{8B}(t) = kC_{8B} \times C_8(t)$	$P_x(\Omega_X) = k_X(\Omega_X - 1)^{nx} \times C_x \times A_{ss} \times A_{rs} \times I_p \times I_o$
$CF_{8O}(t) = kC_{8O} \times C_8(t)$	For $\Omega_X < 1$,
$CF_{Ou1}(t) = kC_{Ou1} \times C_O(t)$	$D_x(\Omega_X) = k_X(1 - \Omega_X)^{nx} \times C_x \times A_{ss} \times A_{rs} \times I_p \times I_o$
$CF_{R1}(t) = kC_{R1} \times C_R(t)$	$P_x(\Omega_X) = 0$
$CF_{R2,\,DOC}(t) = kC_{R2,\,DOC} \times C_R(t)$	
$CF_{R2,\,POC}(t) = kC_{R2,\,POC} \times C_R(t)$	C_x = mass of carbonate mineral under consideration; A_{ss} = specific surface area; A_{rs} = reactive surface area; I_p = phosphate inhibition;
$CF_{R4}(t) = kC_{R4} \times C_R(t)$	I_o = organic matter inhibition.
$CF_{R5}(t) = kC_{R5} \times C_R(t)$	

than the carbonate chemistry. However, we chose to investigate this relationship in order to cover the full range of possible effects on biogenic calcification arising from decreasing seawater carbonate saturation state.

The dependence of biogenic calcification on temperature is also given by two different relationships in *SOCM*. In the first case, a negative parabolic relationship between calcification rate and temperature was assumed based on experimental results for the coral *Pocillopora damicornis* (Clausen and Roth, 1975), and the coralline alga *Porolithon gardineri* (Agegian, ms, 1985; Mackenzie and Agegian, 1989). Although the latter was based on extension rates rather than actual calcification rates, the relationship between temperature and calcification rate or extension rate from the two studies are very similar when normalized to the maximum rate of calcification and maximum extension rate. The relationship adopted that describes the rate of calcification as a function of temperature is:

$$R_T = 100 - 1.32\Delta T^2, \tag{6}$$

where R_T is the relative rate of calcification expressed as a percentage of the rate at the initial temperature in the year 1700 and ΔT is the temperature change in degrees Celsius. A recent study of two species of scleractinian corals shows a similar trend of calcification rate versus temperature (Marshall and Clode, 2004), although the parabolic trend of this study is more convex than that used in *SOCM,* indicating that changes in temperature could have an even larger effect on the rate of calcification than our model calculations show. It also should be emphasized that the calculated rates of calcification are positive even though the adopted relationship is termed negative parabolic. In the second case, a positive linear relationship was obtained from the observed rates of calcification of multiple coral colonies from the Great Barrier Reef, Hawaii and Thailand (Grigg, 1982, 1997; Scoffin and others, 1992; Lough and Barnes, 2000):

$$R_T = 100 + 28\Delta T \tag{7}$$

There are some potential problems with applying this relationship, which are discussed in the *Effect of surface water temperature* section. The overall equation describing the flux of biogenic carbonate production (F) is:

$$F = k \times C_{DIC} \times \frac{R_{\Omega,t}}{R_{\Omega,t=0}} \times \frac{R_{T,t}}{R_{T,t=0}}, \tag{8}$$

where F is the flux of carbon in mol yr^{-1}, k is the rate constant based on the initial flux and the initial reservoir size (see eq 3), C_{DIC} is the total mass of DIC in the surface water in mol C, and R_Ω and R_T are the relative rates of calcification as a function of carbonate saturation state and temperature, as given in equations (4) to (7).

Inorganic dissolution and precipitation.—Inorganic dissolution (R_d) and precipitation (R_p) of carbonate minerals within the pore water–sediment system are described by kinetic rate equations of the general form:

$$R_d = k_d(1 - \Omega)^{n_d}, \tag{9}$$

and,

$$R_p = k_p(\Omega - 1)^{n_p}, \tag{10}$$

where k_d is the rate constant for dissolution and k_p is the rate constant for precipitation, Ω the pore water carbonate saturation state, and n_d *and* n_p the reaction order for dissolution and precipitation, respectively (table 2). The constant parameters were obtained from the experimental results of Zhong and Mucci (1989) for precipitation,

TABLE 2

Adopted constants for inorganic $CaCO_3$ precipitation and dissolution rates (R)

Precipitation $R = k(\Omega-1)^n$ (Zhong and Mucci, 1989)	Rate constant (k) (μmol m^{-2} h^{-1})	Reaction order (n)
Calcite	$10^{-0.29}$	2.80
15 mol% Mg-calcite*	$10^{-0.29}$	2.80
Aragonite	$10^{1.09}$	2.36
Dissolution $R = k(1-\Omega)^n$ (Walter and Morse, 1985)	**(μmol g^{-1} h^{-1})**	
Calcite	$10^{2.82}$	2.86
15 mol% Mg-calcite	$10^{2.62}$	3.34
Aragonite	$10^{2.89}$	2.48

*Assuming same rate as calcite.

and Walter and Morse (1985) for dissolution. The reaction rates were calculated based on the total mass of calcium carbonate in the sediments by converting the calculated rates per unit area to mass per unit time using average specific surface areas (0.1-0.5 m^2 g^{-1}) and the ratio between reactive surface area and total area (0.003-0.66) for typical shallow-water biogenic sediment components (Walter and Morse, 1984, 1985). Inhibition by dissolved phosphate (10 μmol L^{-1}) and dissolved organic matter (10 mg kg^{-1}) (Morse and others, 1985) was also taken into account following the work of Berner and others (1978) by multiplying the rate equations by inhibition factors corresponding to these concentrations (table 1) (Andersson, ms, 2003). Because pore water chemistry is significantly heterogeneous spatially and the reaction kinetics of carbonate minerals in the natural environment are poorly known, sensitivity analyses (the *Sensitivity Analyses* section) were used to evaluate if the above assumptions were realistic relative to the global estimates of total calcium carbonate production and dissolution.

Air–sea CO_2 exchange.—For a coastal ocean water reservoir, as shown in figure 1, the balance of dissolved inorganic carbon (DIC) is the difference between its inputs and outputs as fluxes $F\times$1yr, where fluxes are in units of mol C per year:

$$\Delta DIC = F_{DIC\ inflow} - F_{DIC\ outflow} - F_{CaCO_3\ ppt} + F_{CaCO_3\ diss} - F_{GPP} + F_R + F_{CO_2} \qquad (11)$$

The organic carbon balance is expressed, similarly to that of DIC:

$$\Delta C_{org} = F_{Corg\ inflow} - F_{Corg\ outflow} + F_{GPP} - F_R - F_{Corg\ S} \qquad (12)$$

The sum of (11) and (12), with the notation of $\Delta DIC = [DIC_{eq}] - [DIC_0]$, is:

$$[DIC_{eq}] - [DIC_0] = F_{DIC\ inflow} - F_{DIC\ outflow} - F_{CaCO_3\ ppt} + F_{CaCO_3\ diss} + (F_{Corg\ inflow} - F_{Corg\ outflow} - F_{Corg\ S} - \Delta C_{org}) + F_{CO_2} \qquad (13)$$

The individual terms in equations (11) to (13) and their initial values at the end of pre-industrial time, taken as the year 1700 (Andersson, ms, 2003), are (fig. 1):

- $[DIC_{eq}]$ is the DIC concentration at equilibrium with atmospheric CO_2 after all the other input and removal fluxes have been accounted for. The value of DIC_{eq} depends on (1) the atmospheric CO_2 concentration and (2) a change in total alkalinity of seawater due to the net input of alkalinity via rivers, runoff and upwelling, and precipitation and dissolution of $CaCO_3$. $[DIC_0]$ is the initial DIC concentration (2000 μmol kg^{-1}).

- $F_{\text{DIC inflow}}$ is the DIC input from land and by upwelling from deeper ocean to the coastal ocean (1536.2×10^{12} mol C yr^{-1}) and $F_{\text{DIC outflow}}$ is its output by water exchange with the open ocean (1503×10^{12} mol C yr^{-1}); $F_{\text{Corg inflow}}$ ($26 + 8 = 34 \times 10^{12}$ mol C yr^{-1}) and $F_{\text{Corg outflow}}$ (18×10^{12} mol C yr^{-1}) are the inflows and outflows, respectively, of organic carbon that consists of dissolved organic carbon (DOC), living biota, and particulate detritus; $F_{\text{Corg S}}$ is the permanent burial and net organic carbon storage rate in sediments, taken here as 9×10^{12} mol C yr^{-1} (see Mackenzie and others, 2004a).
- $F_{\text{CaCO}_3\text{ ppt}}$ is precipitation of $CaCO_3$ from biological and/or inorganic processes (24.5×10^{12} mol C yr^{-1});
- $F_{\text{CaCO}_3\text{ diss}}$ is dissolution of $CaCO_3$ minerals (6×10^{12} mol C yr^{-1});
- F_{GPP} is the consumption of CO_2 in gross primary production (600×10^{12} mol C yr^{-1});
- F_{R} is the production of CO_2 by autotrophic and heterotrophic respiration of organic carbon that includes C_{org} from external inputs and from *in situ* primary production (607×10^{12} mol C yr^{-1});
- F_{CO_2} is the air-sea CO_2 flux, taken as negative for a flow from seawater to the atmosphere (that is, coastal water is a CO_2 source) and positive for transfer from the atmosphere (that is, coastal water is a CO_2 sink) (-21.7×10^{12} mol C yr^{-1}).

The CO_2 air-sea flux (F_{CO_2}) in equation (13) is negative when CO_2 is emitted from coastal water, making the coastal water a source of CO_2 to the atmosphere, and it is positive when the coastal zone is a CO_2 sink. With this notation, equation (13) can be written in the following form:

$$F_{CO_2} = (F_{\text{DIC outflow}} - F_{\text{DIC inflow}}) + (F_{\text{CaCO}_3\text{ ppt}} - F_{\text{CaCO}_3\text{ diss}}) + (F_{\text{Corg outflow}} + F_{\text{Corg S}} - F_{\text{Corg inflow}} + \Delta C_{org}) + \Delta DIC. \quad (14)$$

Because the surface water is assumed to attain equilibrium with the atmosphere instantaneously, ΔDIC is effectively the time rate of change of total dissolved inorganic carbon content (C_{DIC}) of the surface water, dC_{DIC}/dt, as a function of changes in the inorganic carbon content of the atmosphere (C_{ATM}). The relationship is essentially a modification of the Revelle-Munk function and can be derived from the following expression:

$$\frac{dC_{\text{DIC}}}{dt} = \frac{d}{dt}\left[C_{\text{DIC},t=0}\left\{ \frac{(C_{ATM} - C_{ATM,t=0})}{(R_0 + C_{ATM,t=0} + D(C_{ATM} - C_{ATM,t=0}))} + 1 \right\}\right] \quad (15)$$

The Revelle constant (D) was taken as 4, and the factor R_0 as 9. The latter value indicates that the buffer mechanism of seawater causes a fractional rise of CO_2 in the surface water that is one ninth of the increase in the atmosphere (Bacastow and Keeling, 1973; Revelle and Munk, 1977; Ver, ms, 1998).

At the onset of the simulation, the shallow-water ocean environment was set to be a net source of CO_2 to the atmosphere of -21.7×10^{12} mol C yr^{-1} (fig. 1) owing to the assumption that this region was net heterotrophic at this time by -7×10^{12} mol C yr^{-1} (Smith and Mackenzie, 1987; Wollast and Mackenzie, 1989; Smith and Hollibaugh, 1993; Mackenzie and others, 1998; Mackenzie and others, 2004b) and because of calcium carbonate production of 24.5×10^{12} mol C yr^{-1} (Milliman, 1993; Milliman and Droxler, 1996), resulting in a release of -14.7×10^{12} mol C yr^{-1} to the atmosphere assuming that 0.6 mol of CO_2 is released to the atmosphere for every mol $CaCO_3$ precipitated (Smith, 1985; Ware and others, 1992; Frankignoulle and others, 1994; Lerman and Mackenzie, 2004, 2005). It is customary to write the precipitation reaction of $CaCO_3$ in seawater or fresh water as:

$$Ca^{2+} + 2HCO_3^- = CaCO_3 + CO_2 + H_2O \quad (16)$$

Thus for every two moles of HCO_3^- removed from the aqueous solution, one mole of $CaCO_3$ is precipitated and one mole of CO_2 is released back to the solution and eventually escapes to the atmosphere as gaseous CO_2. However, as Smith (1985) has shown, the stoichiometry of this reaction is only correct for a relatively low pH fresh water solution but not for seawater. Surface seawater is a slightly basic solution with a pH of about 8.2. It has a relatively high carbonate buffer capacity and seawater pH decreases only slightly in response to $CaCO_3$ precipitation. The CO_2 that is formed as a result of the precipitation of $CaCO_3$ reacts with the water and leads to a reapportionment of the H^+, HCO_3^-, and CO_3^{2-} ions and H_2CO_3 (CO_{2aq}) in the seawater. Because of this, at 25°C and a pCO_2 of $10^{-3.5}$ atm, the CO_2 gas loss from the seawater is only about 60 percent as large as the dissolved inorganic carbon incorporated into the solid phase $CaCO_3$. The remaining 40 percent of the carbon enters the DIC pool of seawater. Smith (1985) also showed that the released CO_2 is probably incorporated into organic matter so that the net reaction for the precipitation of $CaCO_3$ and the fate of the carbon that enters the DIC pool of seawater is:

$$Ca^{2+} + 2HCO_3^- = CaCO_3 + CH_2O + O_2 \quad (17)$$

Frankignoulle and others (1994) and Lerman and Mackenzie (2004, 2005) subsequently showed that the amount of the gaseous CO_2 that escapes seawater because of the precipitation of $CaCO_3$ is variable and dependent on several environmental factors including temperature, salinity, atmospheric CO_2 concentration, DIC speciation, and the rate at which the $CaCO_3$ precipitates from the water. The ratio of CO_2 released from seawater of normal salinity to $CaCO_3$ removed by precipitation is 0.51 to 0.66 mol/mol, between 15° and 25°C, and the atmospheric CO_2 concentration between the pre-industrial 280 ppmv and the early 21st century 375 ppmv (Lerman and Mackenzie, 2005).

Based on the above considerations, our model partitions the carbon released to seawater upon the precipitation of $CaCO_3$ as 60 percent gaseous release to the atmosphere and 40 percent incorporation into the DIC pool of seawater, which is a boundary condition of the model and the CO_2 flux equation at the initial quasi-steady state (fig. 1). This assumption implies that at steady state for every 2 mol HCO_3^- brought in via rivers and upwelling and every mol $CaCO_3$ precipitated, 0.6 mol of C is released to the atmosphere and 0.4 mol of C is fixed into organic matter or exported to the open ocean. Although we recognize that the partitioning of CO_2 released owing to calcification varies as a function of the previously described parameters, we did not vary this parameter throughout the model simulation runs. Taking into account the partitioning of CO_2 from $CaCO_3$ production (fig. 1), as discussed above, and the resulting change in DIC from equation (15), the final CO_2 flux relationship that is given in equation (14) can be written as:

$$\begin{aligned} F_{CO_2} &= -0.6 \times F_{CaCO_3\ ppt} + [(F_{DIC\ outflow} - F_{DIC\ inflow}) + (2F_{CaCO_3\ ppt} - 0.4 \times F_{CaCO_3\ ppt} \\ &\quad - F_{CaCO_3\ diss}) + (F_{Corg\ outflow} + F_{CorgS} - F_{Corg\ inflow} + \Delta C_{org}) + dC_{DIC}/dt] \\ &= (F_{DIC\ outflow} - F_{DIC\ inflow}) + (F_{CaCO_3\ ppt} - F_{CaCO_3\ diss}) \\ &\quad + (F_{Corg\ outflow}, + F_{CorgS} - F_{Corg\ inflow} + \Delta C_{org}) + dC_{DIC}/dt \\ &= (F_{DIC\ outflow} - F_{DIC\ inflow}) + NEC + NEM^* + dC_{DIC}/dt \end{aligned} \quad (18)$$

where *NEC* is the net ecosystem calcification ($CaCO_3$ production flux − dissolution flux) and *NEM** is the net ecosystem metabolism which is defined as (Andersson and Mackenzie, 2004; Mackenzie and others, 2004b):

$$NEM^* = F_{GPP} - F_R = F_{Corg\ outflow} + F_{Corg\ S} - F_{Corg\ inflow} + \Delta C_{org} \quad (19)$$

At the onset of simulation in the year 1700, equation (18) yields (in 10^{12} mol C yr^{-1}):

$$F_{CO_2} = (1503 - \{32 + 1504.2\}) + (24.5 - 6) + (18 + 9 - 26 - 8) + 0 = -21.7 \quad (20)$$

Bearing in mind the uncertainties of the flux estimates that are given in the literature and in figure 1, the calculated CO_2 emission of -21.7×10^{12} mol C yr^{-1} is in very good agreement with the result of $-21 \pm 5 \times 10^{12}$ mol C yr^{-1}, obtained from the CO_2 air–sea transfer model of Lerman and Mackenzie (2005) over a range of temperature and other environmental conditions that takes into account inflows and outflows of DIC and reactive C_{org}, as well as the formation and net storage of $CaCO_3$ and C_{org} in sediments.

Dissolved Inorganic Carbon (DIC) System Calculations

DIC system calculations in *SOCM* were done for 25°C and 35 psu based on pCO_2 and total DIC for both surface water and pore water. Calculations were carried out thermodynamically (Morse and Mackenzie, 1990) adopting total ion activity coefficients in seawater at 25°C and 35 psu (Millero and Pierrot, 1998), and the first and second dissociation constants of the carbonic acid system from Plummer and Busenberg (1982). Although calcium and magnesium concentrations have been observed to deviate from their predicted conservative proportions in certain coastal regions and within pore waters, these proportions were assumed to remain constant in *SOCM*. Calcium carbonate solubilities (K_{sp}) for calcite and aragonite are the values of Plummer and Busenberg (1982), and those of magnesian calcite solubility are from Bischoff and others (1987, 1993). In order to compare the results to observational seawater data, the DIC system was recalculated based on pCO_2 and DIC derived from the model and the stoichiometric carbonic acid system constants defined by Mehrbach and others (1973) and refit by Dickson and Millero (1987) using the program CO2SYS (Lewis and Wallace, 1998). For details on the solubility constants of calcite and aragonite adopted in these calculations see Lewis and Wallace (1998).

Sensitivity Analyses

In order to investigate the initial assumptions, the robustness of the results, and the relative importance of various parameters adopted in *SOCM,* multiple sensitivity analyses were conducted. The one-at-a-time sensitivity method was used, changing one parameter at a time while holding all others equal to their values for the base-case scenario (Hamby, 1994). The sensitivity of each parameter was obtained numerically by using the maximum absolute ratio of variation index (MAROV) (Dubus and Brown, 2002):

$$\mathrm{MAROV} = \mathrm{Max}\left|\frac{(O - O_{BC})}{(I - I_{BC})} \times \frac{I_{BC}}{O_{BC}}\right| \quad (21)$$

where O is the output value, O_{BC} is the output value for the base-case scenario, I is the input value, and I_{BC} is the original input value for the base-case scenario. The larger the resulting MAROV index for a parameter, the larger the potential influence of that parameter on model output. If MAROV = 1, changes in the input parameter by X percent will at most result in the same variation in the output parameter.

External Forcings

The major forcings of the model, as shown in figure 2, are atmospheric CO_2 concentration, variations in the global average surface temperature, and organic

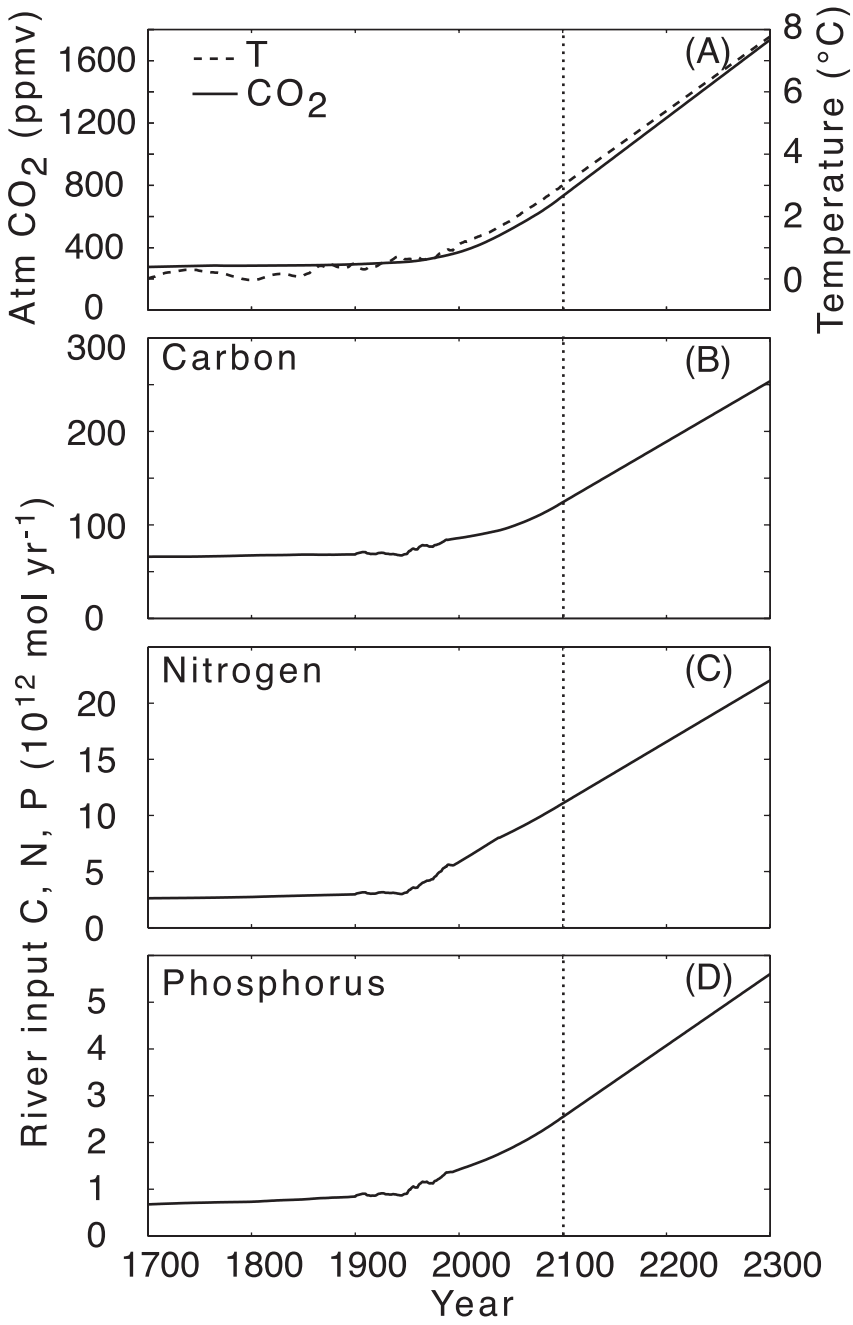

Fig. 2. Major forcings of *SOCM*. (A) Atmospheric CO_2 concentration and temperature change according to observational data and the International Panel on Climate Change "business–as–usual" emission scenario (IPCC IS92a) (Enting and others, 1995; Houghton and others, 1996, 2001), linearly extrapolated beyond the year 2100. River inputs of (B) carbon (reactive particulate organic carbon, refractive particulate organic carbon, dissolved organic carbon, dissolved inorganic carbon), (C) nitrogen (reactive particulate organic nitrogen, refractive particulate organic nitrogen, dissolved organic nitrogen, dissolved inorganic nitrogen, particulate inorganic nitrogen), and (D) phosphorus (reactive particulate organic phosphorus, refractive particulate organic phosphorus, dissolved organic phosphorus, dissolved inorganic phosphorus, particulate inorganic phosphorus) based on observational data and model predictions using the Terrestrial Ocean aTmosphere Ecosystem Model (*TOTEM*) (see for example, Ver and others, 1999a) until 2025. Beyond this year, the data were linearly extrapolated in the base–case scenario until 2100 and in the long–term scenario until 2300.

matter and nutrient inputs to the coastal ocean. Atmospheric CO_2 concentrations and temperature are according to historical records and the IPCC IS92a scenario until the year 2100 (Enting and others, 1995; Houghton and others, 1996, 2001). Inputs of organic and inorganic carbon and nutrients (N and P) via rivers and runoff, and upwelling are based on observational data (Meybeck, 1982; Meybeck and Ragu, 1995, 1997) and model predictions from the Terrestrial Ocean aTmosphere Ecosystem Model (*TOTEM,* references given in the INTRODUCTION) until the year 2025 and linearly extrapolated thereafter. As mentioned previously, the *TOTEM* results for the continental output from land and groundwaters via rivers to the ocean are used as input to SOCM. At the initial condition of the model simulation in the year 1700, the input and output fluxes of C, N, and P were assumed to be balanced and the shallow-water ocean environment was considered to be in a quasi-steady state. At this time, the carbon material balance is consistent with a coastal water residence time of 4 years. Numerical simulations were also employed beyond the year 2100 adopting a hypothetical forcing scenario with respect to fossil fuel emissions, nutrient and organic matter export via rivers, and upwelling from deep waters (see subsequent discussion on the century scale future of the coastal carbonate system).

BIOGEOCHEMICAL CONSEQUENCES OF INCREASING ATMOSPHERIC CO_2

In the subsections to follow, the effects of increasing CO_2 on seawater chemistry, marine calcifying organisms and ecosystems, and the pore water-sediment system are presented and discussed. In order to highlight the potential consequences of increasing atmospheric CO_2, model results of *SOCM* until the year 2100 are presented first in conjunction with background information and theory, observational data and discussion.

Seawater Chemistry

As the atmospheric concentration of CO_2 increases, the flux of this gas into the surface ocean will also increase owing to Henry's law that expresses the solubility of CO_2 in seawater: $[CO_2\ (aq)] = K_0^* \times pCO_2$, where K_0^* is the stoichiometric solubility coefficient. The dissolved CO_2 will react with water and form aqueous CO_2 and carbonic acid, which will dissociate into bicarbonate, carbonate and hydrogen ions:

$$CO_2 + H_2O = H_2CO_3 = H^+ + HCO_3^- = 2H^+ + CO_3^{2-} \qquad (22)$$

The net result of this process can be illustrated by the simplified reaction:

$$CO_2 + H_2O + CO_3^{2-} = 2HCO_3^- \qquad (23)$$

which demonstrates how an increase in CO_2 essentially titrates carbonate ions to form bicarbonate ions. As a consequence, the CO_2 concentration in solution changes only slightly because of the buffering effect of the carbonate ions. However, reaction (22) results in an increase in the H^+-ion concentration and a decrease in the pH. The relative increase in total DIC is not proportional to the relative increase in CO_2, but is approximately only 10 percent of the relative CO_2 increase. Furthermore, as the partial pressure of CO_2 increases, the relative increase in DIC becomes smaller and consequently the CO_2 buffer capacity of seawater also decreases. Because dissolution of $CaCO_3$ minerals produces carbonate ions, the CO_2 buffer capacity of seawater could be enhanced by this process that is discussed in more detail later.

The results of *SOCM* suggest that the global coastal ocean has served as a net source of CO_2 to the atmosphere throughout most of the past 300 years owing to the process of calcification and a state of net heterotrophy, which leads to generation of CO_2 (fig. 3) (Andersson and Mackenzie, 2004; Mackenzie and others, 2004b). However, the role of this region has recently switched, or soon will do so, to a net sink of

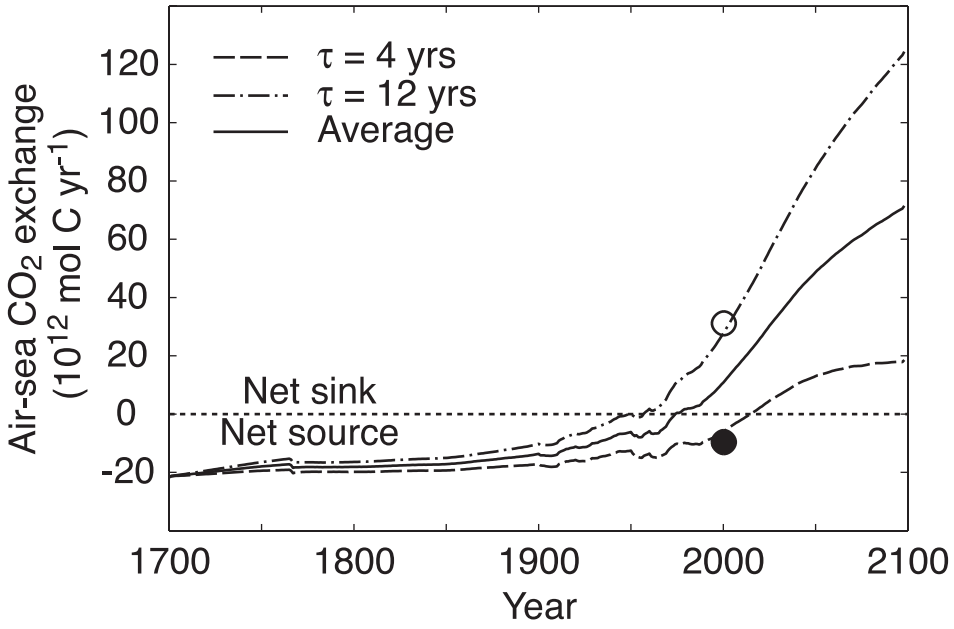

Fig. 3. Net air–sea CO_2 exchange (10^{12} mol C yr^{-1}) between 1700 and 2100 calculated by *SOCM* adopting an average coastal water residence time (τ) of 4 years and 12 years. The solid line indicates the average flux of the two scenarios. The data points indicate the recent net air-sea CO_2 exchange estimates by Borges (2005) based on observational data from coastal zone ecosystems: coastal zone including estuaries (solid circle) acts as a net source of CO_2, and excluding estuaries (open circle) the coastal region acts as a net sink of CO_2. Note that estuaries ($\sim 1 \times 10^6$ km^2) constitute less than 4% of the global coastal region ($\sim 28 \times 10^6$ km^2).

CO_2 because of rising atmospheric CO_2 and potentially increasing inorganic nutrient loading from land that stimulates new production and net autotrophy. In the present model simulations, the CO_2 flux is significantly dependent on the term [$F_{\text{DIC outflow}} - F_{\text{DIC inflow}}$] in equation (18), which represents a small difference between two very large fluxes that are not well known, but can be defined based on a material balance. As a consequence, the flux of CO_2 is strongly affected by the initial carbon material balance and the residence time of water in the coastal ocean. In previously published results, the difference between these large flux terms had been taken to be approximately zero because of the uncertainty associated with the terms and did not affect the air-sea CO_2 exchange substantially.

Our current model projections of the net air-sea CO_2 exchange agree well with recent estimates by Borges (2005) based on CO_2 flux data from different coastal environments extrapolated to the global coastal region. Including estuaries, Borges concluded that the global coastal region currently serves as a net source of CO_2 to the atmosphere of approximately -10×10^{12} mol C yr^{-1}, which agrees relatively well with the estimate by *SOCM* of -6×10^{12} mol C yr^{-1} for the year 2000 (fig. 3), adopting a relatively long coastal ocean water residence time of 12 years (fig. 1, DIC mass/$F_{\text{DIC outflow}} = 6000 \times 10^{12}$ mol C/480×10^{12} mol C $yr^{-1} \approx 12$ yr). However, if estuaries were not included, Borges' result is that the global coastal region serves as a net sink of CO_2 equivalent to approximately $+30 \times 10^{12}$ mol C yr^{-1} (fig. 3), which agrees well with the results of *SOCM* adopting a shorter, and probably more reasonable, residence time of approximately 4 years ($F_{\text{DIC outflow}} = 1503 \times 10^{12}$ mol C yr^{-1}). Based on recent estimates of continental margin and coastal upwelling rates (Chavez and Toggweiler,

1995), the average residence time of water within the global coastal region is approximately 2 to 3 years. However, it should be pointed out that substantial uncertainty is associated with any generalization of the global coastal region, which is highly variable and heterogeneous in both time and space. There is a strong need for more long-term time series data from coastal environments in order to pin down the behavior of the global and individual coastal zone environments relative to air-sea CO_2 exchange.

In the model simulation of *SOCM,* both gross primary production and total ecosystem respiration increased owing to increasing inputs of inorganic nutrients and organic matter from land to the coastal ocean. Although the numerical results indicate that the increase in organic matter primary production (consumption of CO_2) has been roughly balanced by a similar increase in total ecosystem respiration (production of CO_2) up until the present, future projections of the model suggest that nutrient input and gross primary production will continue to increase and progressively exceed land organic matter input and total remineralization in coastal waters, leading to increased net autotrophy. Increased autotrophy implies increased storage of organic matter within the global coastal region and/or increased export of organic matter to the open ocean, and thereby also enhancement of the potential role of the coastal ocean as a sink for atmospheric CO_2. Even if the export of organic matter and nutrients from land to the coastal ocean were different, and this region instead became increasingly heterotrophic, it is still very likely that the global coastal ocean would become a significant sink of CO_2 owing to the rapid increase of CO_2 in the atmosphere (Ver and others, 1999b; Mackenzie and others, 2004a).

As mentioned earlier in this section, increasing atmospheric CO_2 results in an overall decrease in the pH and carbonate ion concentration. A decrease in carbonate ion concentration will result in a decrease in the seawater saturation state (Ω) with respect to carbonate minerals such as calcite and aragonite, the degree of which is determined by the following relationship:

$$\Omega = \frac{[Ca^{2+}][CO_3^{2-}]}{K_{sp}^*} \tag{24}$$

where K_{sp}^* denotes the stoichiometric solubility product, and $[Ca^{2+}]$ and $[CO_3^{2-}]$ are total concentrations of calcium and carbonate ions, respectively. Because calcium concentration is nearly constant in the ocean and is by a factor of about 30 to 50 greater than the concentration of the carbonate ion in surface water, the saturation state is mainly controlled by the abundance of this anion. If $\Omega > 1$ the solution is said to be supersaturated and if $\Omega < 1$ the solution is undersaturated with respect to the carbonate phase under consideration. From a thermodynamic perspective, one would expect a carbonate phase to precipitate if $\Omega > 1$ and dissolve if $\Omega < 1$. However, this is strictly not always the case because of kinetic constraints and inhibition by various components of seawater, such as magnesium and phosphate ions and dissolved organic matter (see for example, Berner and others, 1978; Morse, 1983; Morse and Mackenzie, 1990). As an example, most surface waters are supersaturated with respect to calcite by 5 to 6 times, but no significant abiotic precipitation of carbonate minerals is observed other than in a very few environments such as the Great Bahama bank and the Persian Gulf (Morse and Mackenzie, 1990). Instead, most calcium carbonate is of biological origin, produced by marine organisms that manufacture their skeletons, shells, and tests out of calcium carbonate. As discussed in the next section, a decrease in surface water carbonate saturation state might have significant implications for carbonate secreting organisms such as corals, coralline algae, foraminifera, and coccolithophorids.

As anticipated due to the increase in atmospheric CO_2, the dissolved inorganic carbon concentration of seawater has already been observed to increase in surface

waters at the locations of the Hawaiian Ocean Time series (HOT) (Winn and others, 1998; Hawaii Ocean Time series, 2004) and the Bermuda Atlantic Time–Series (BATS) (Bates and others, 1996; Bates, 2001), located in the North Pacific subtropical gyre and the North Atlantic subtropical gyre, respectively. The surface water carbonate saturation state has also decreased at these locations (fig. 4). In addition, recent observations from open ocean environments have shown a shoaling of the carbonate saturation horizon in several regions of all major ocean basins (Feely and others, 2004).

The results of *SOCM* suggest that the carbonate saturation state of the surface water of the global coastal ocean may decrease by 46 percent between the year 1700 and year 2100 (fig. 4). The surface water will remain supersaturated with respect to both aragonite and calcite in the year 2100, and in metastable equilibrium with a magnesian calcite phase with $MgCO_3$ content greater than 20 mol percent adopting the solubilities of Bischoff and others (1987, 1993). At high latitudes the saturation state with respect to these phases will be lower and the seawater possibly even undersaturated with respect to aragonite and many magnesian calcite phases. The trend predicted by the model simulation agrees with results by other investigators (Kleypas and others, 1999; McNeil and others, 2004), and also with surface water observations from the Hawaiian Ocean Time series between 1989 and 2001 (fig. 4) (Hawaii Ocean Time series, 2004). If one incorporates data from nearby stations of the GEOSECS cruise in 1973 (Takahashi and others, 1980) and the CO_2 dynamics cruise in 1981 (Chen and others, 1986), a consistent decline in surface water carbonate saturation state can be seen in the North Pacific subtropical gyre in figure 4. One must be cautious in the interpretation of the trend line because the locations of these sampling programs differ and the marine carbon system was analyzed by different laboratories at different times. A decreasing carbonate saturation state trend is also seen in inshore data from Mangrove Bay, Bermuda, for the years 1979 to 2004 (fig. 4). However, care also must be taken in interpreting these data because they were obtained by different investigators, there are few data points, and there is substantial spatial and temporal heterogeneity of the marine carbon system that is characteristic of inshore environments. Nevertheless, it should be kept in mind that a decrease in carbonate saturation state for this environment is what we would anticipate due to the significant increase observed in atmospheric CO_2.

Marine Calcifying Organisms and Ecosystems

Effect of calcium carbonate saturation state.—Increasing atmospheric CO_2 and subsequent decreasing surface water carbonate saturation state may have a negative effect on marine calcifying organisms because their ability to calcify is dependent on the carbonate saturation state. Numerous experimental investigations have demonstrated the existence of a direct relationship between the rate of calcification and seawater carbonate saturation state or pCO_2 for a number of different calcifying organisms such as coccolithophorids (Riebesell and others, 2000; Zondervan and others, 2001; Sciandra and others, 2003), foraminifera (Spero and others, 1997; Bijma and others, 1999, 2002), coralline algae (Smith and Roth, 1979; Borowitzka, 1981; Agegian, ms, 1985; Mackenzie and Agegian, 1989; Gao and others, 1993), and scleractinian corals (Gattuso and others, 1998; Marubini and Thake, 1999; Marubini and others, 2001, 2003; Reynaud and others, 2003). In addition, experiments on typical calcareous communities have been conducted in incubation chambers and mesocosms (Halley and Yates, 2000; Leclercq and others, 2000, 2002), and on the artificial reef of Biosphere 2 (fig. 5) (Langdon and others, 2000, 2003). Although substantial variations have been observed between species and communities, the major results and conclusions of most studies have been similar: the rate of calcification has been observed to decrease as a function of decreasing carbonate saturation state or increasing pCO_2. Based on these experimental results and future projections of surface water carbonate saturation, marine

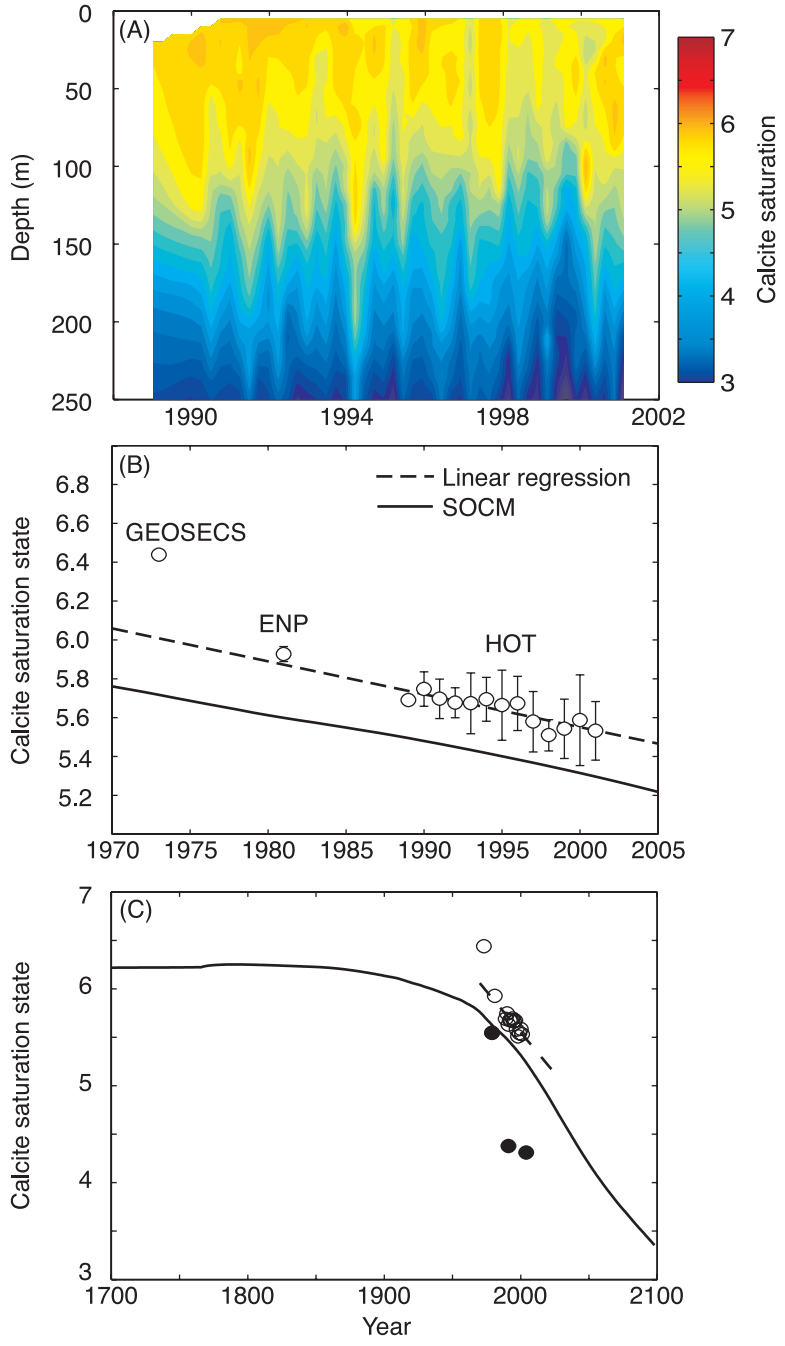

Fig. 4. (A) Contour plot of seawater calcite saturation state between 0 and 250 meters depth from the Hawaiian Ocean Time series (HOT) at station ALOHA in the North Pacific subtropical gyre between 1989 and 2001. The calcite saturation state is indicated by the scale bar to the right of the plot. (B) Average annual surface water calcite saturation state (open circles) at station ALOHA (HOT, 2004) and single measurements taken at nearby stations during the CO_2 dynamics cruise in 1981 (ENP) (Chen and others, 1986) and the GEOSECS cruise in 1973 (Takahashi and others, 1980). The error bars indicate one standard deviation. Because the exact locations differ and the carbonate system was analyzed by different investigators, the linear regression is only based on the data from HOT (dashed line: $y = -0.0252t + 56.1284$; $R^2 = 0.82$; $p << 0.01$).

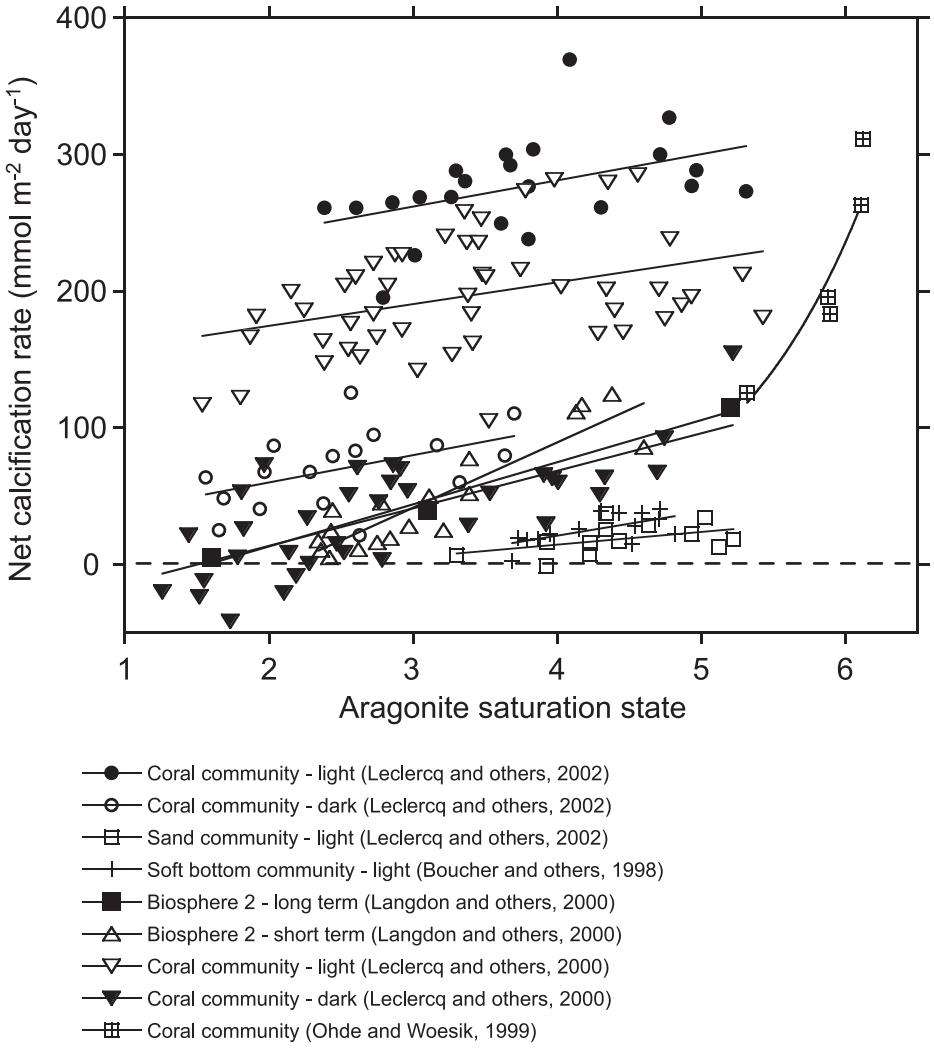

Fig. 5. Community net calcification rate as a function of aragonite saturation state under different environmental conditions adopted from the references cited in figure. Positive values represent net precipitation and negative values represent net dissolution of carbonate minerals. Solid lines represent the best linear fit to the data except for the data of Ohde and Woesik (1999), which are represented by a power equation.

biogenic calcification may decrease by 11 to 44 percent owing to a doubling of the atmospheric CO_2 concentration relative to pre-industrial conditions (Gattuso and others, 1999; Langdon, 2002; Buddemeier and others, 2004). The question that

---

The solid line indicates the surface water calcite saturation state projected by *SOCM*. The same data are shown in (C) together with inshore data from Mangrove Bay, Bermuda (solid circles) and the projection by *SOCM* between 1700 and 2100. The dissolved inorganic carbon system and calcite saturation state were calculated at *in situ* temperature and salinity in each case from either total alkalinity or pCO_2 together with total DIC using the program CO2SYS (Lewis and Wallace, 1998) and the carbonate dissociation constants of Mehrbach and others (1973), refit by Dickson and Millero (1987). For details on the solubility constant of calcite adopted in the calculation see Lewis and Wallace (1998).

remains to be answered is whether lower carbonate saturation state and decreased rates of calcification will negatively affect corals and other calcifying organisms ecologically. In order to resolve this issue, we require an understanding of the mechanisms of calcification and the function of calcification in calcifying organisms. Obvious advantages include functions such as structural support and protection from predators and desiccation, as well as increased surface area, but other hypotheses suggest that calcification may facilitate nutrient and/or bicarbonate uptake (McConnaughey and Whelan, 1997; McConnaughey and others, 2000; Cohen and McConnaughey, 2003).

As a result of lower surface water carbonate saturation state, one hypothesis suggests that the physical strength and structure of the skeletons, shells and tests deposited by marine calcifiers may become weaker and more susceptible to environmental stress in general, both natural and anthropogenic (Kleypas and others, 1999, 2001; Buddemeier and others, 2004). As a consequence, calcareous organisms may not thrive in a world characterized by high CO_2 and low carbonate saturation state and may be at a competitive disadvantage in their environment relative to other non-calcifying organisms that occupy the same habitats. For example, it would be anticipated that coral reef habitats might experience a successive transition from being dominated by corals and coralline algae to being dominated by seaweeds and fleshy macro algae. A recent report from the Caribbean indicates that the average hard coral cover on reefs in this region has declined from 50 percent to 10 percent in the last three decades (Gardner and others, 2003). Although local factors, both natural and anthropogenic, such as disease, storms, temperature stress, predation, over-fishing, sedimentation, eutrophication, and habitat destruction were attributed to the observed decline, the effect of decreasing carbonate saturation state cannot be ruled out as a co-factor. Numerous worldwide observations report similar significant declines in coral reef health, which along with future climate projections has lead to the proclamation of a global "coral reef crisis" (Buddemeier and others, 2004).

Based on current experimental results and the observed increase in atmospheric CO_2 since the onset of the industrial revolution, one would expect the rate of calcification of marine calcifying organisms to have already declined by 6 to 14 percent (Kleypas and others, 1999; Buddemeier and others, 2004). However, no observations of such a decline exist at this time. On the contrary, analyses of drill cores taken from *Porites* colonies along the Great Barrier Reef suggest that the rate of calcification of these corals has increased rather than decreased between 1880 and the later part of the 20th century (Lough and Barnes, 2000). Similar results showing increased calcification rates toward the present have also been obtained from a coral core taken in French Polynesia (Bessat and Buiges, 2001). However, it is important to recognize that the rate of calcification is not singularly controlled by carbonate saturation state, but also strongly related to other parameters such as temperature that is discussed in the next section, light (Marubini and others, 2001), nutrients (Paasche and Brubak, 1994; Marubini and Atkinson, 1999; Ferrier–Pagès and others, 2000; Sciandra and others, 2003), and metabolic and photosynthetic activity of the organism if the organism is autotrophic or dependent on autotrophic symbionts. Lough and Barnes (2000) attributed the observed increase in calcification on the Great Barrier Reef to an increase in the average annual sea surface temperature during the 20th century and concluded that calcification rates have significantly increased in response to global warming. An increase in biogenic calcification during this time was also observed in *SOCM* simulations adopting a positive but unlikely linear temperature dependence (eq 7; see discussion in next section), as well as in scenarios adopting a curvilinear saturation state dependence (eq 5; fig. 6). In the former, the positive effect of increasing temperature outweighed the negative effect of decreasing carbonate satura-

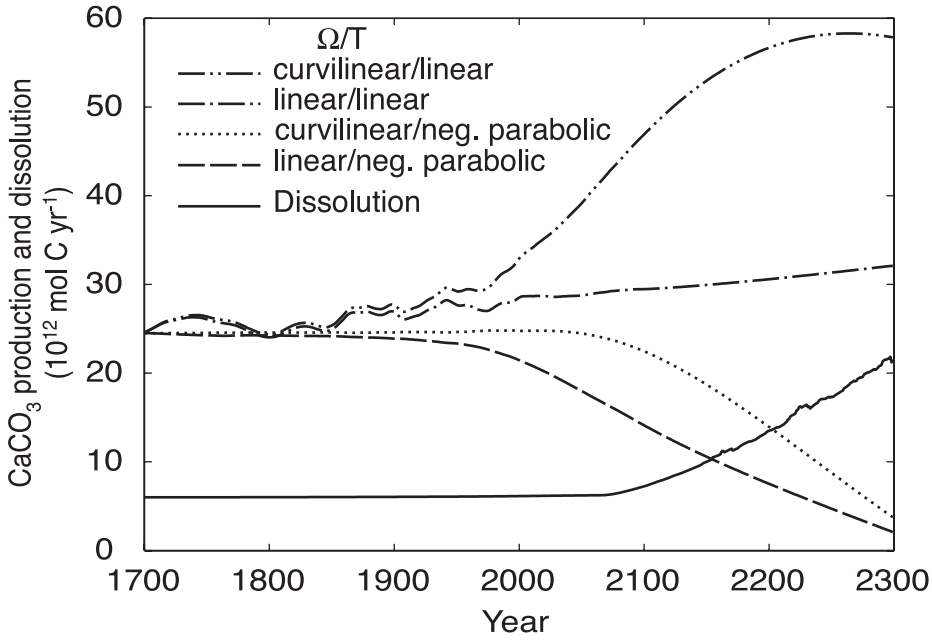

Fig. 6. $CaCO_3$ dissolution and biogenic $CaCO_3$ production between 1700 and 2300 adopting different combinations of the dependence of calcification on saturation state (Ω) [curvilinear or linear; equations (4) and (5)] and temperature (T) [negative parabolic or linear; equations (6) and (7)] adopting the forcing scenario shown in figure 2. Although the results are shown adopting a linear temperature dependence, we are hesitant to adopt this as a functional relationship between calcification and temperature (see discussion in text) and it should be viewed with caution.

tion state on the rate of calcification. The observed increase in the latter combined with a negative parabolic temperature dependence was due to increasing DIC and not temperature. However, once the surface water carbonate saturation state became lower than a certain threshold in the second half of the 21st century, the negative effect of this decrease became more important than the positive effect of increasing DIC and the rate of calcification significantly decreased in the model simulations.

Effect of surface water temperature.—Based on data from different geographical locations characterized by different annual average sea surface temperatures (Hawaiian archipelago: Grigg, 1982, 1997; Phuket, Thailand: Scoffin and others, 1992; Great Barrier Reef: Lough and Barnes, 2000), Lough and Barnes (2000) concluded that a positive linear relationship exists between the rate of calcification and sea surface temperature for the species of the coral genus *Porites*. In contrast to these conclusions, experimental results on individual coral colonies and coralline algae suggest that a negative parabolic relationship exists between the rate of calcification and temperature, indicating an upper temperature limit for the maximum rate of calcification (Clausen and Roth, 1975; Agegian, ms, 1985; Mackenzie and Agegian, 1989; Marshall and Clode, 2004). Future projections on how calcification rates will be affected in the future by decreasing carbonate saturation state and increasing temperature are significantly different depending on whether one accepts a positive linear (eq 7) or a negative parabolic (eq 6) temperature relationship. The results of *SOCM* suggest that global shallow–water carbonate production could either increase by almost 70 percent or decrease by approximately 44 percent by the year 2100 depending on the temperature and saturation state relationships adopted in the model (fig. 6). Similar projec-

tions made by McNeil and others (2004), adopting a positive linear temperature and a positive linear saturation state dependence, suggest that net coral calcification significantly increases between the years 1900 and 2100 by approximately 40 percent as the positive effect of ocean warming outweighs the negative effect of decreasing carbonate saturation state. Although the results of McNeil and others (2004) agree with one trend predicted from *SOCM* simulations adopting a positive linear temperature-calcification relationship, there is little reason to conclude that the predicted trend derived from this linear relationship is valid (see Kleypas and others, 2005, for a detailed discussion on the problems associated with this relationship). Corals and other marine calcifyers are currently living at their upper threshold limit for temperature and increasing seawater temperature during El Niño events has resulted in bleaching of corals and coral mortality in the Atlantic Ocean, Caribbean Sea, and Pacific Ocean (Buddemeier and others, 2004; Kleypas and others, 2005). Thus, the linear relationship is presented here simply to provide completeness to the model simulations.

The positive linear relationship observed between coral calcification and the average annual temperature in different geographic locations is most likely due to increased metabolism and/or increased photosynthetic activity by symbiotic zooxanthellae (Buddemeier and others, 2004). However, another factor that may affect the rate of calcification is the carbonate ion concentration that varies as a function of temperature and latitude (Mackenzie and others, 1983). In addition, modern corals have evolved in their environment for thousands of years or longer under relatively constant temperature conditions, allowing them to adapt or acclimate to the prevailing regional climate conditions. Consequently, the response of marine calcifying organisms to increasing sea surface temperature may depend not only on the amount of the temperature increase but also on the rate of that increase. It also should be pointed out that the temperature of the tropics might not change strongly although the global average temperature may increase significantly as a result of global warming (Houghton and others, 2001). Thus, the effect of temperature on coral calcification rates could turn out to be relatively small.

In calcifying organisms hosting symbiotic algae, photosynthesis and calcification are strongly coupled. Calcification rates are approximately three times higher in light conditions when photosynthesis is active than in the dark when this process is inactive (Gattuso and others, 1999). It has been suggested that primary production in some algae may be limited by CO_2 concentration (Riebesell and others, 1993; Raven, 1993, 1997). If carbon fixation by symbiotic algae is limited by the availability of CO_2, photosynthesis and consequently calcification may increase in the future owing to increasing concentrations of CO_2, and the negative effect of decreasing carbonate saturation state would then partly be counteracted by the increase in photosynthetic activity (Leclercq and others, 2002). However, there is currently no conclusive evidence confirming that the primary production of coral reef ecosystems is limited by the availability of CO_2. Thus, it is most likely that an increase in primary production of coral reefs and other carbonate communities owing to increasing CO_2 will not significantly compensate for a decrease in calcification rate. Furthermore, calcification rate versus carbonate saturation state experiments include both zooxanthellae and the animal host; that is both the symbiont and the host are affected by the changes in seawater chemistry, and the net result is that calcification declines regardless of the response in primary production.

Pore Water–Sediment System: Carbonate Chemistry and Mineral Dissolution

Ultimately, decreasing surface water and/or pore water carbonate saturation state could lead to dissolution of carbonate minerals and affect the average carbonate mineral composition and the rate of formation of carbonate cements in the pore

water–sediment system (Garrels and Wollast, 1978; Mackenzie and Agegian, 1989; Morse and Mackenzie, 1990; Andersson and others, 2003). Because carbonate cements function as the glue for reef structures, any changes to their content and/or composition could affect the strength and ability of a reef to withstand environmental stress. In addition, the increased dissolution of metastable carbonate minerals would increase the CO_2 buffer capacity of the ocean according to equation (23). In fact, such dissolution has been proposed to act as a buffer to neutralize anthropogenic CO_2 uptake by the ocean and prevent any negative effects of rising atmospheric CO_2 on calcareous organisms and carbonate systems (Garrels and Mackenzie, 1980; Barnes and Cuff, 2000; Halley and Yates, 2000).

The results of *SOCM* suggest that dissolution of carbonate minerals is likely to increase in the future, but will not produce sufficient surface water alkalinity to restore to a significant extent any changes in pH and carbonate saturation state in the global coastal ocean owing to increasing atmospheric CO_2. In the model simulations, the observed increase in carbonate dissolution is the result of a decrease in pore water carbonate saturation state and not that of the surface water, which remained supersaturated with respect to the average magnesian calcite phase of 15 mol percent $MgCO_3$ by the year 2100. Further discussion of the solubilities of magnesian calcites and their occurrences is given in the DISCUSSION OF 600 YEARS OF THE CO_2–CARBONATE SYSTEM section. The modeled decrease in pore water carbonate saturation state was not due to increasing atmospheric CO_2, but rather due to increasing transport, deposition and subsequent remineralization of organic matter in the global coastal zone sediments. Sensitivity results adopting different IPCC atmospheric CO_2 scenarios (IS92a, B1, A1Fl) (Houghton and others, 2001) showed that pore water carbonate chemistry was little affected by changes in the surface water carbonate chemistry (fig. 7). Sensitivity results also indicated that the extent of carbonate dissolution was mainly controlled by microbial remineralization of organic matter rather than carbonate reaction kinetics (table 3) (Morse and Mackenzie, 1990).

The results of the MAROV analysis demonstrated that the reaction rate constant (k) and reaction order (n) had a small influence on the extent of carbonate dissolution relative to the influence of organic matter decay, although the reaction order was more important than the rate constant (table 3). Hence, the continuous decomposition of organic matter by microbes, releasing CO_2 and maintaining a low carbonate saturation state within the sediment-pore water system, which drives dissolution of carbonate minerals, is the major factor controlling the extent of calcium carbonate dissolved. This process has been well demonstrated as occurring under aerobic conditions in the pore waters of sediments from the Gulf of Calvi, Corsica, by Moulin and others (1985). Furthermore, the results of the MAROV analysis show that the stoichiometric solubility product was the most sensitive parameter and had the largest influence on the extent of carbonate dissolution. Nevertheless, this result does not add any variability to the model results with respect to aragonite and calcite because the solubilities of these minerals are well constrained. On the other hand, considerable uncertainty and controversy are associated with the solubility of magnesian calcite minerals and especially on how these minerals behave in the natural environment, as is discussed in more detail in the DISCUSSION OF 600 YEARS OF THE CO_2–CARBONATE SYSTEM section. Except for the magnesian calcite stoichiometric solubility product and organic matter decomposition, other parameters investigated using the MAROV index had a relatively small influence on the model results (table 3).

In the simulations of *SOCM,* the pore water became undersaturated with respect to the average magnesian calcite phase of 15 mol percent $MgCO_3$ in the year 2065. This phase was then subject to dissolution. The substantial increase in dissolution with respect to this phase was observed as a buffering effect within the pore water (fig. 8).

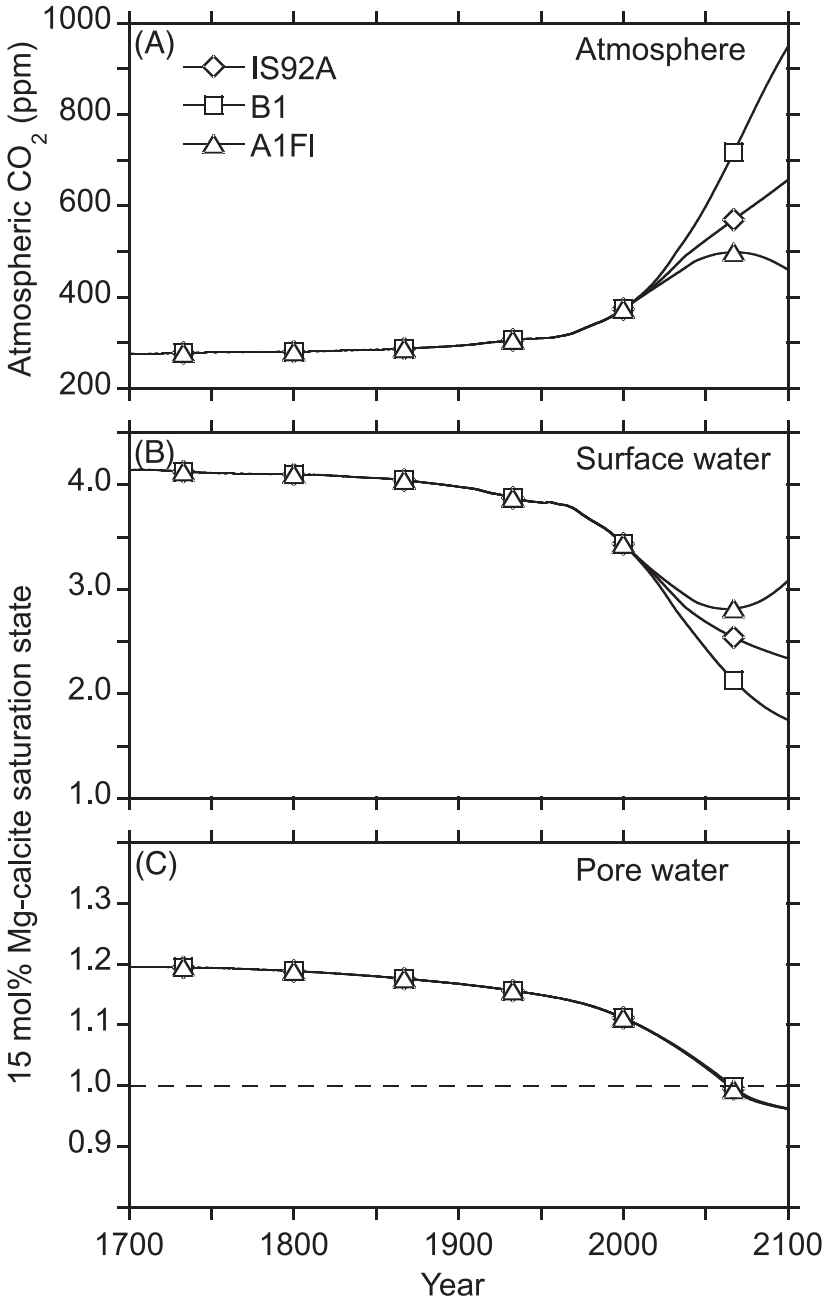

Fig. 7. (A) Atmospheric CO_2 concentration projected by *TOTEM* according to IPCC emission scenarios IS92a, B1 and A1Fl and, (B) resulting surface water, and (C) pore water saturation state with respect to 15 mol % magnesian calcite calculated at 25°C and 35 psu using the atmospheric CO_2 concentrations in (A) as forcings in *SOCM*. Although the surface water carbonate saturation state is significantly affected by different atmospheric CO_2 concentrations, the pore water carbonate saturation state is little affected by these changes. Note also that the surface water saturation state remains supersaturated with respect to the average 15 mol % magnesian calcite phase by the end of the 21st century in all scenarios.

TABLE 3

Relative sensitivity of various parameters on $CaCO_3$ dissolution in SOCM according to the MAROV index (Dubus and Brown, 2002). The higher the value of the index, the more sensitive is the parameter.

Parameter	$CaCO_3$ dissolution	
	MAROV	Rank
Ion activity product	55.282	1
Organic matter remineralization	14.296	2
Initial DIC chemistry	2.431	3
Magnesian calcite composition	0.760	4
Reaction order (n)	0.225	5
Initial $CaCO_3$ mass	0.111	6
Inhibition factor	0.002	7
Reaction rate constant (k)	0.000	8

Although the average pore water did not become undersaturated with respect to this phase until near the end of the simulation, the pore water was already undersaturated with respect to magnesian calcite compositions with greater mol percent $MgCO_3$ and thus these phases were subject to dissolution before this event (fig. 8). If an average magnesian calcite phase of 20 mol percent $MgCO_3$ were adopted in the model at the initial conditions, the pore water would become undersaturated with respect to this phase already in the first half of the 20th century. Consequently, the average $MgCO_3$ content of magnesian calcite cements and the bulk magnesium content of contemporary carbonate sediments could gradually decrease as an effect of changes in the average pore-water saturation state.

In *SOCM,* the average pore-water saturation state changed from an initial metastable equilibrium with 21 mol percent to 14 mol percent $MgCO_3$ by the year 2100 assuming that no significant buffer effect was produced owing to dissolution by magnesian calcite minerals with a $MgCO_3$ content >15 mol percent. The results suggest that the activity of carbonate ions in the pore water is controlled by a metastable equilibrium between the pore water and the most soluble solid carbonate phase present within the sediments. During early diagenesis on the seafloor, dissolution of carbonate minerals follows a sequence based on mineral thermodynamic stability, progressively leading to removal of the more soluble phases until the most stable phases remain (fig. 8). Such selective dissolution of metastable carbonate minerals has been observed both in experimental and natural environments (Chave, 1962; Schmalz and Chave, 1963; Neumann, 1965; Wollast and others, 1980; Balzer and Wefer, 1981; Morse and Mackenzie, 1990; Halley and Yates, 2000; Leclercq and others, 2002). For example, observations from carbonate sediments in Bermuda follow a trend of increasing carbonate mineral stability with decreasing grain size, which most likely indicates selective dissolution (Chave, 1962; Schmalz and Chave, 1963; Neumann, 1965). However, caution is advised in interpretation of this trend because it may be influenced by the biogenic source and size of the material. Simple saturometry experiments have also demonstrated selective dissolution to occur in the water column of Devil's Hole, Bermuda (Balzer and Wefer, 1981), where substantial dissolution of carbonate minerals occurs as a result of extensive remineralization of organic matter below the seasonal thermocline during summer, producing elevated levels of CO_2 and low carbonate saturation state (fig. 9).

According to Halley and Yates (2000), the rate of carbonate dissolution in coral reef environments could equal the rate of calcification once atmospheric CO_2 concentrations reached approximately 2 times pre–industrial levels causing a slowdown or

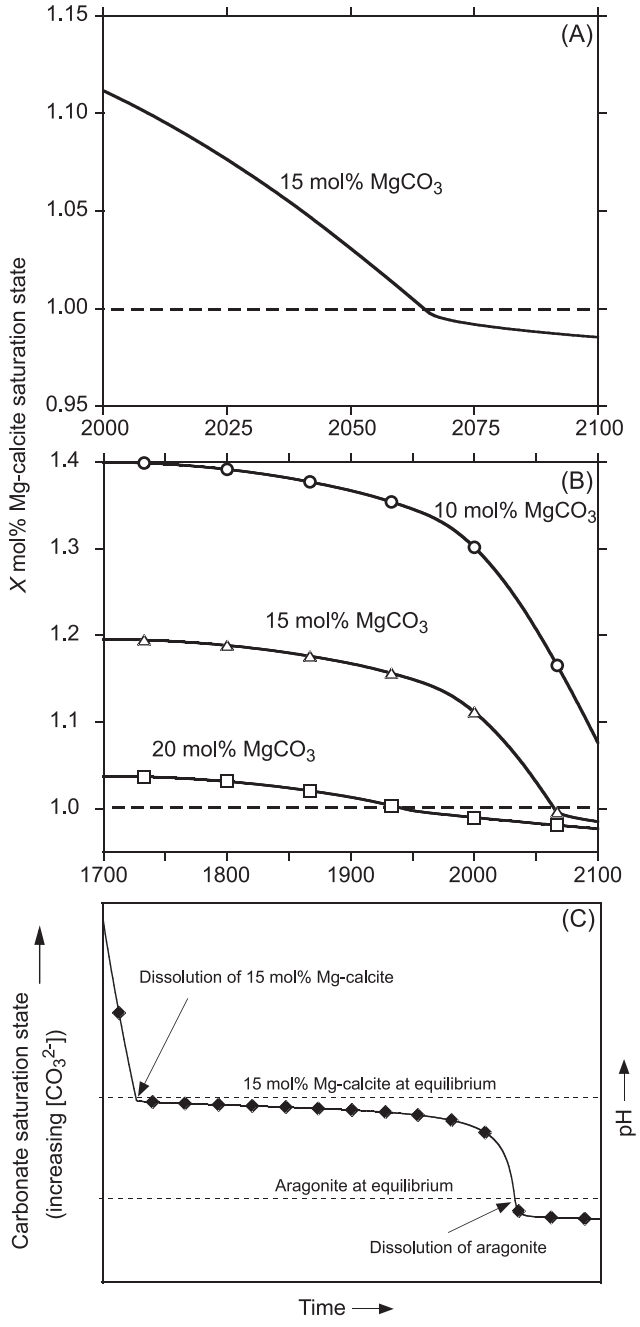

Fig. 8. (A) Pore water saturation state with respect to 15 mol % magnesian calcite between 2000 and 2100 calculated at 25°C and 35 psu. An apparent buffer effect of the pore water is observed upon dissolution of this carbonate phase in the latter part of the 21st century. (B) Pore water saturation state with respect to a range of magnesian calcite phases using different average magnesian calcite compositions (10, 15, 20 mol % $MgCO_3$) in the model. In the standard scenario of *SOCM*, the metastable equilibrium between pore water and a magnesian calcite composition changed from 21 to 14 mol % magnesian calcite. (C) Hypothetical scenario illustrating how the carbonate ion concentration is controlled by a metastable equilibrium between the pore water and the most soluble solid carbonate phase present in the sediments. Initially, a decrease in carbonate saturation state is observed until dissolution of 15 mol % magnesian calcite is initiated. At this

reversal in the loss of reef structures because of the buildup of alkalinity in seawater (Buddemeier and others, 2004). Opposed to these conclusions, the results of *SOCM* show that pore water carbonate chemistry and dissolution rates of carbonate minerals are not significantly affected by future projected changes in surface water carbonate chemistry (see preceding discussion). This model finding is in agreement with the conclusions of Leclercq and others (2002), based on mesocosm experiments, that changes in surface water pH and carbonate saturation state have little effect on the pH and carbonate saturation state of interstitial waters, which is mainly controlled by microbial processes within the pore water–sediment system. Furthermore, the model results of *SOCM* showed that the carbonate saturation state of the surface water of the shallow-water ocean environment is above saturation with respect to the average magnesian calcite phase of 15 mol percent $MgCO_3$ by the end of the simulation in the year 2100. Thus dissolution of $CaCO_3$ minerals in the global coastal ocean will mainly be controlled by changes in deposition and subsequent remineralization of labile organic matter rather than the projected changes in the surface water carbonate chemistry during the 21st century. In addition, a substantial, but unknown fraction of calcium carbonate dissolution can be attributed to biological erosion (Hutchings, 1986; Kleypas and others, 2001).

Surface Water Buffering Owing to Carbonate Dissolution

Global coastal environment.—If the mass of carbonate minerals dissolved in the water column or sediments of the coastal ocean were substantial and the alkalinity from the dissolution process ultimately came to reside in the water column, the seawater carbonate system could be buffered because of the heterogeneous chemical reaction involving seawater, atmospheric CO_2 gas and carbonate minerals. The rate of change of pH owing to the heterogeneous reaction would be slower than that due to the simple homogeneous chemical reaction involving solution of atmospheric CO_2 into the coastal ocean surface waters. However, even if the rate of dissolution were to equal the rate of $CaCO_3$ production (Halley and Yates, 2000; Buddemeier and others, 2004), the results of *SOCM* indicate that dissolution of metastable carbonate minerals will not produce sufficient alkalinity to restore any changes in pH and carbonate saturation state owing to increasing atmospheric CO_2. In order to buffer the surface water pH and carbonate saturation state against rising atmospheric CO_2, dissolution of $CaCO_3$ minerals in the global surface ocean essentially has to balance the net invasion of anthropogenic CO_2 ($\sim 170 \times 10^{12}$ mol C yr^{-1}). Even if dissolution of $CaCO_3$ in the surface sediment layer were equal to the current rates of global $CaCO_3$ production ($\sim 95 \times 10^{12}$ mol C yr^{-1}) (Wollast, 1994), the surface water would still only be partially buffered. However, dissolution rates of this magnitude are very unlikely since most of the $CaCO_3$ produced in pelagic environments ($\sim 70 \times 10^{12}$ mol C yr^{-1}) (Wollast, 1994) sinks and dissolves at deeper depths because surface waters are oversaturated with most carbonate minerals (Milliman and others, 1999). Thus because the physical exchange of water between the shallow–water ocean environment and the open ocean is relatively fast and the residence time short (2 to 3 years) (Chavez and Toggweiler, 1995), substantial dissolution of metastable carbonate minerals within this region is necessary to produce sufficient alkalinity to counteract any changes in the surface water chemistry owing to increasing atmospheric CO_2. Current estimates of $CaCO_3$ dissolution in the global coastal ocean range from 6.7×10^{12} mol C yr^{-1} (Milliman,

stage, the pore water is buffered and maintained close to metastable equilibrium with this phase. The metastable equilibrium persists until the phase has completely dissolved. The carbonate saturation state decreases until a new equilibrium state is established with the next phase (in this case aragonite). The calculation assumes Ca^{2+} and Mg^{2+} concentrations remain constant in the pore water.

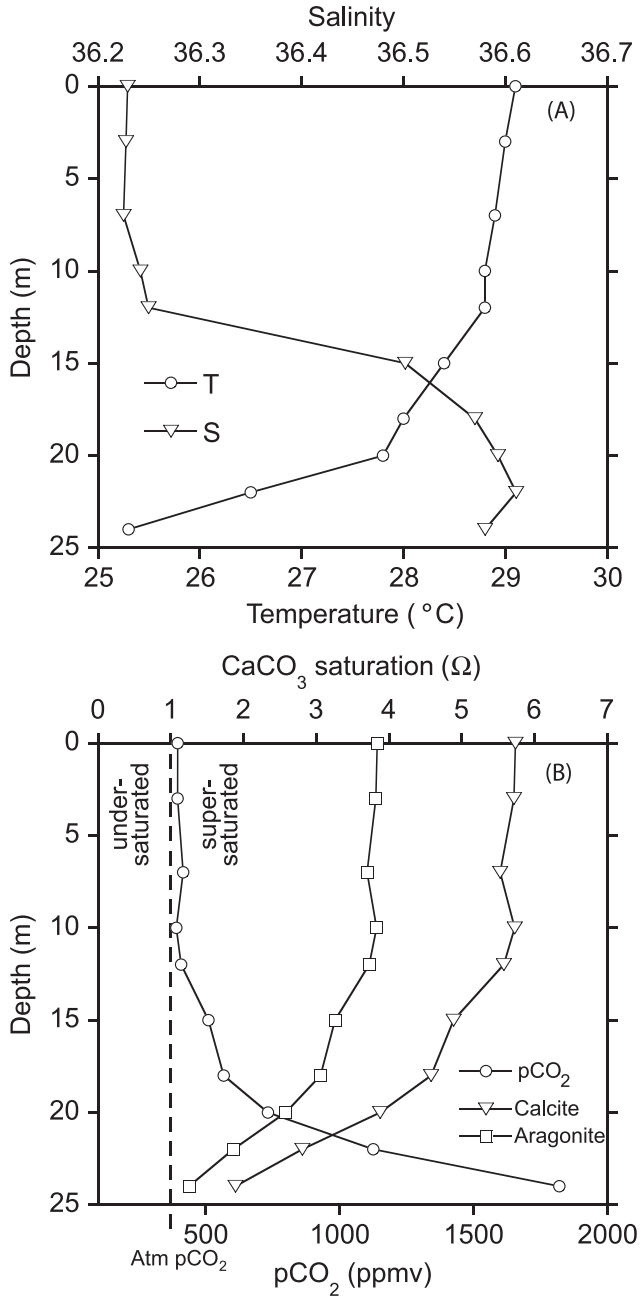

Fig. 9. Vertical water column profiles during summer time at Devil's Hole, Bermuda, showing (A) temperature and salinity, and (B) CO_2 partial pressure and saturation state with respect to calcite and aragonite calculated at *in situ* temperature and salinity according to the procedure described in figure 4. Extensive remineralization of organic matter below the thermocline releases CO_2 resulting in high pCO_2 and low carbonate saturation state, which drives dissolution of metastable carbonate minerals and virtual absence of magnesian calcite phases in the carbonate muds of Devils's Hole (Neumann, 1965).

1993) to 10×10^{12} mol C yr^{-1} (Langdon, 2002), the higher estimate corresponding to about 6 percent of the average net anthropogenic invasion of CO_2 into the global ocean during the 1980s ($\sim 160 \times 10^{12}$ mol C yr^{-1}) (Sarmiento and Gruber, 2002). However, according to Langdon (2002), direct measurements of carbonate dissolution range from 0 to 13.7 mmol $CaCO_3$ m^{-2} day^{-1}, which if extrapolated to the entire shallow–water ocean environment corresponds to 0 to 140×10^{12} mol C yr^{-1}. Dissolution of this magnitude is more than 5 times the amount of $CaCO_3$ produced annually within the global coastal ocean (24.5×10^{12} mol C yr^{-1}) (Milliman, 1993; Milliman and Droxler, 1996) and implies a substantial loss of calcium carbonate minerals from reef structures and sediments. Langdon (2002) also pointed out that a dissolution rate of 17 mmol $CaCO_3$ m^{-2} day^{-1} ($\sim 170 \times 10^{12}$ mol C yr^{-1}) is necessary to balance the current invasion of anthropogenic CO_2, an estimate that will increase as atmospheric CO_2 continues to rise.

Regional environments.—In addition to the extent and rate of carbonate dissolution, which is mainly controlled by remineralization of organic matter (*Pore Water-Sediment System: Carbonate Chemistry and Mineral Distribution* section) (Morse and Mackenzie, 1990) and to some extent biological erosion, *SOCM* sensitivity results indicate that the rate of physical water exchange with the open ocean significantly influences the extent of buffering observed in the surface water of the shallow–water ocean environment. If the rate of dissolution is rapid enough and the residence time is long enough, a buffer effect could be observed in some regions, such as certain lagoons with restricted circulation, but not on a global scale. In an attempt to investigate the effects of increasing atmospheric CO_2 and subsequent carbonate dissolution on a regional scale, the conceptual framework of *SOCM* was used to construct a model representative of the global coral reef area (600×10^6 km^2) (Smith, 1978). The average water depth of this region was assumed to be 30 meters. Conceptually, the model is essentially identical to *SOCM* except for the parameterization of reservoir masses, fluxes and forcings (Voluer, ms, 2004). Most of the parameterizations were obtained from estimates in the literature pertinent to coral reef environments, but if sufficient data were not available, parameters were proportionally downscaled from *SOCM* (table 4). The main objective of the regional version of *SOCM* was to investigate the influence of residence time and physical exchange with the open ocean on the surface water buffer effect produced by dissolution of metastable carbonate minerals. Multiple sensitivity analyses were conducted with respect to the residence time of water ranging from as short as five days to a maximum of a year. Actual residence times of different coral reef environments (mainly atolls) in the Pacific Ocean range from less than a day to approximately six years (table 5) (DeLesalle and Sournia, 1992).

The results of the analysis demonstrate that increasing residence times allow for a stronger buffer effect owing to dissolution of carbonate minerals in the sediments, resulting in greater neutralization of invading anthropogenic CO_2 and consequently higher surface water carbonate saturation state at the end of the simulation in the year 2100 (fig. 10). Hence, the increase in alkalinity and buffer capacity produced from dissolution of calcium carbonate is not diluted as rapidly if the water exchange with the open ocean is relatively slow and the water residence time longer. Furthermore, the results indicate that biogenic calcification is not as severely affected by increasing atmospheric CO_2 in carbonate environments with longer residence times because the carbonate saturation state is not depressed as much as in regions with shorter residence times, assuming everything else is held constant. However, it should be pointed out that present-day reef growth is most vigorous where water residence time is short, as on shelf-edge reefs and outer rims of atolls, rather than where it is long, as on inner-shelf reefs and in atoll lagoons.

Table 4

Initial mass and quasi-steady state flux estimates of the regional version of SOCM (Voluer, ms, 2004)

Reservoir	10^{12} mol C
Surface water	35.6
Surface water organic matter	1.3
Pore water	1.14
Sediment organic matter	1000
Sediment calcite	882
Sediment aragonite	4438
Sediment magnesian calcite	1680
Flux	**10^{12} mol C yr^{-1}**
River/runoff DIC	0.64
River/runoff DOC	0.36
River/runoff reactive POC	0.16
River/runoff refractive POC	0.16
Biological production	55
Respiration	52.4
Organic matter sedimentation	1.36
Organic matter burial	0.3
Organic matter export to open ocean	1.76
Organic matter remineralization	1.22
Biogenic calcification	9
Air-sea CO_2 exchange (negative = net evasion)	-4
$CaCO_3$ burial	7.2
$CaCO_3$ export to open ocean	0.9
Net abiotic precipitation and dissolution (negative = net dissolution)	-0.9
Surface water pore water exchange	4.32
Surface water open ocean exchange	68
Upwelling/onwelling	78.44

The century-scale future of the coastal carbonate system

In this section we address the behavior of the CO_2-carbonic acid-carbonate system in the coastal ocean beyond the year 2100, the year at which the IPCC ends its

Table 5

Water residence times at different coral reef locations in the South Pacific Ocean

Lagoon	Location	Island type	# of passes	Residence Time (days)
Tiahura	Moorea Island	high island	1	0.25
Tarawa	Kiribati	atoll	1	12
Fangataufa	Tuamotu	atoll	1	16
Moruroa	Tuamotu	atoll	1	23
Fanning	Line Islands	atoll	3	32
Enewetak	Marshall Islands	atoll	3	33
Mataiva	Tuamotu	atoll	1	40
Canton	Pheonix Islands	atoll	1	50
Tikehau	Tuamotu	atoll	1	170
Takapoto	Tuamotu	atoll	0	2190

Adopted from Voluer (ms, 2004) modified from Delesalle and Sournia (1992).

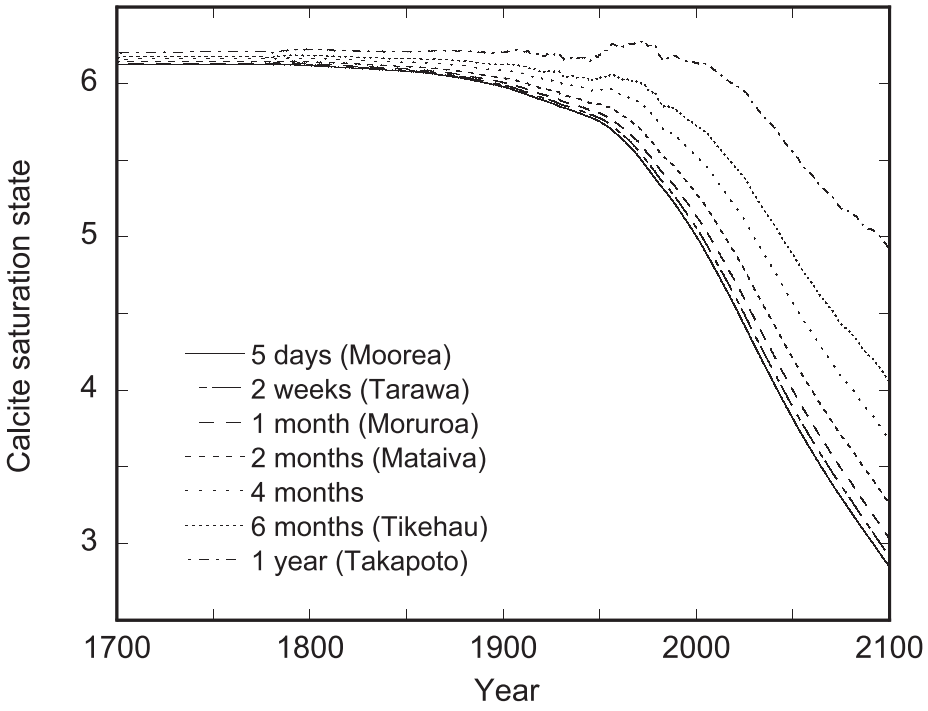

Fig. 10. Surface water calcite saturation state in the regional version of *SOCM* adopting different water residence times (see text). Examples of atolls in the Pacific Ocean with similar residence times are shown in parenthesis (table 5) (Delesalle and Sournia, 1992). The longer the residence time, the stronger the carbonate buffer effect and the higher the surface water carbonate saturation state owing to dissolution of metastable carbonate minerals.

atmospheric CO_2 and temperature projections. We recognize the problems inherent in any model predictions of this nature but the fact that both the *TOTEM* and *SOCM* model calculations are supported by the available historical data (Neftel and others, 1985; Friedli and others, 1986; Sarmiento and Sundquist, 1992; Barnola and others, 1995; Etheridge and others, 1996; Keeling and others, 1996; Winn and others, 1998; Keeling and Whorf, 2002; Hawaiian Ocean Time series, 2004; Borges, 2005) encourages us to do so. We consider a model-bounding scenario for the future where atmospheric CO_2 and temperature follow the historical record to the year 2000, then increase according to the IPCC social–economic scenario IS92a to the year 2100 and finally increase linearly from 2100 to 2300. A similar atmospheric CO_2 forcing was employed by Archer and others (1998) in a model study of the long term fate of fossil fuel CO_2 and the role of the ocean and deep-sea carbonate sediments in neutralizing anthropogenic CO_2. Furthermore, in the present modeling scenario, riverine inputs increase according to the output from *TOTEM* from the year 1700 to 2025 and then linearly beyond 2025. This scenario is likely to be an extreme case in terms of changes in inputs of organic and inorganic carbon and nutrients to the coastal ocean. It should be pointed out that there is considerable evidence that the riverine fluxes of organic carbon, nitrogen and phosphorus have increased globally during the past several centuries, perhaps to double their pre-industrial pristine flux values in the year 2000 (Meybeck, 1982, 2001; Mackenzie and others, 2002).

Highlights of Forcing Trends

Figure 2 shows the historical and future trends in the forcing functions of atmospheric CO_2, temperature, and riverine inputs of carbon and nutrients to the coastal ocean starting at the year 1700 and projected to the year 2300 for the model-bounding scenario. The trends from 1700 to 2025 are discussed extensively in Ver and others (1999a, 1999b), Mackenzie and others (2002), and Lerman and others (2004). Note the following for the trends from 2000 to 2300: (1) atmospheric CO_2 increases from about 370 ppmv in the year 2000 to 1730 ppmv in 2300; this represents an increase of almost 2900 Gt of carbon solely in the atmosphere, which is equivalent to approximately 58 percent of the global fossil fuel reserves of coal, oil, and gas (Sundquist, 1985; Kvenvolden, 1988); (2) global mean temperature increases about 6.7°C from 2000 to 2300; and (3) riverine inputs of dissolved inorganic carbon, dissolved organic carbon, labile and non–labile particulate organic carbon, particulate inorganic carbon, each increase by approximately 195 percent, whereas total nitrogen and total phosphorus increase 277 percent and 294 percent, respectively. These forcings are used as inputs to *SOCM* to examine the behavior of CO_2-carbonic acid–carbonate system dynamics and cycling in the coastal ocean.

Results of Model Calculations for Coastal Surface Waters

As anticipated, as atmospheric CO_2 and temperature rise from the year 1700 to 2300, the dissolved inorganic carbon content of coastal zone seawater increases about 17 percent during this period of time (fig. 11). As increasing amounts of CO_2 are absorbed by the coastal ocean, the pH falls and the distribution of marine carbon species changes, resulting in an increase in HCO_3^- and dissolved CO_2 relative to CO_3^{2-}, as follows from equation (23). In concert with this rise in DIC concentration is a decline in the saturation state of seawater with respect to carbonate minerals, mainly due to the decline in the concentration of CO_3^{2-} as it is titrated by carbon dioxide to HCO_3^-, thus lowering the saturation state (eq 24; fig. 11). The saturation state with respect to calcite falls by 73 percent during the 600 years of model numerical simulation where most of the decrease occurs after the year 2000. Because of the decline in saturation state, the rate of biogenic calcification decreases (fig. 6). The decrease in calcification rate amounts to 85 percent to 90 percent of its value in the year 2000, reflecting the adopted saturation state dependence (eqs 4 and 5), and the negative parabolic temperature dependence of the calcification rate (eq 6). This is a substantial reduction and one that, if it were to occur, would have a significant impact on coral reef and other carbonate ecosystems (see the *Effect of calcium carbonate saturation state* section). However, if for completeness of model simulations between the years 2000 and 2300, we adopt a linear temperature-calcification rate dependence (eq 7 and McNeil and others, 2004) and two variants of the saturation-state dependence —the linear (eq 4) and the curvilinear (eq 5)—then the simulations result in an increase in calcification rate from 13 percent to 76 percent, respectively. Nevertheless, it is unlikely that these simulations are realistic representations of the future (see preceding discussion).

Nearly concomitant with the most significant decrease in calcification rate adopting the negative parabolic temperature dependence (eq 6) is an overall increase in the dissolution rate of carbonate suspended particles and sediments (fig. 6). Over the 600 years of the model simulation, the rate of dissolution increases by 260 percent and entails the dissolution mainly of highly soluble magnesian calcite phases, some aragonite, and minor calcite in the sediments. The enhanced dissolution reflects primarily the decrease in carbonate saturation state of the pore waters with respect to carbonate minerals (fig. 12). This decrease in interstitial water saturation state is due to

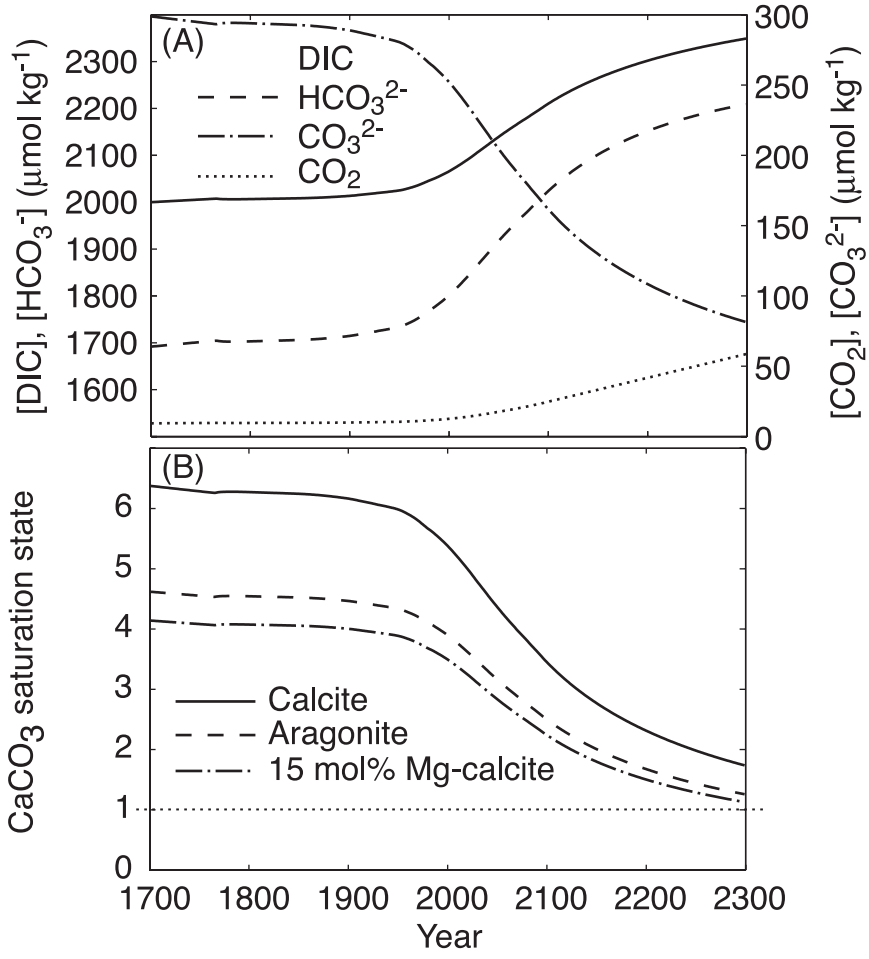

Fig. 11. Surface water dissolved inorganic carbon chemistry between 1700 and 2300 calculated by *SOCM* at 25°C and 35 psu. (A) Total dissolved inorganic carbon concentration [DIC], [CO_2], [HCO_3^-], and [CO_3^{2-}], and (B) surface water saturation state (Ω) with respect to calcite, aragonite and 15 mol % magnesian calcite.

the enhanced sedimentation and remineralization fluxes of organic carbon; the latter provides CO_2 to the sediment–pore water system driving reaction (23) to the right.

Finally, as the coastal ocean is loaded with organic carbon and nutrients during the 600 years of the model simulation, the balance between gross primary production (GPP) and total aerobic and anaerobic respiration, that is net ecosystem metabolism (NEM*), changes (fig. 13). Prior to the year 2000, total respiration exceeds GPP and the system is net heterotrophic (see the *Air-sea CO_2 exchange* and *Seawater Chemistry* sections). After the year 2000, the system becomes increasingly autotrophic, thus acting as a sink of atmospheric CO_2 due to GPP exceeding total respiration. The magnitude of the CO_2 flux due to the imbalance in the year 2300 is equivalent to 52×10^{12} mol C yr^{-1} from the atmosphere to coastal waters (fig. 13). The total coastal ocean air–sea flux at this time is about 172×10^{12} mol C yr^{-1}, reflecting the rise in atmospheric CO_2, the changing organic metabolism imbalance, the declining CO_2

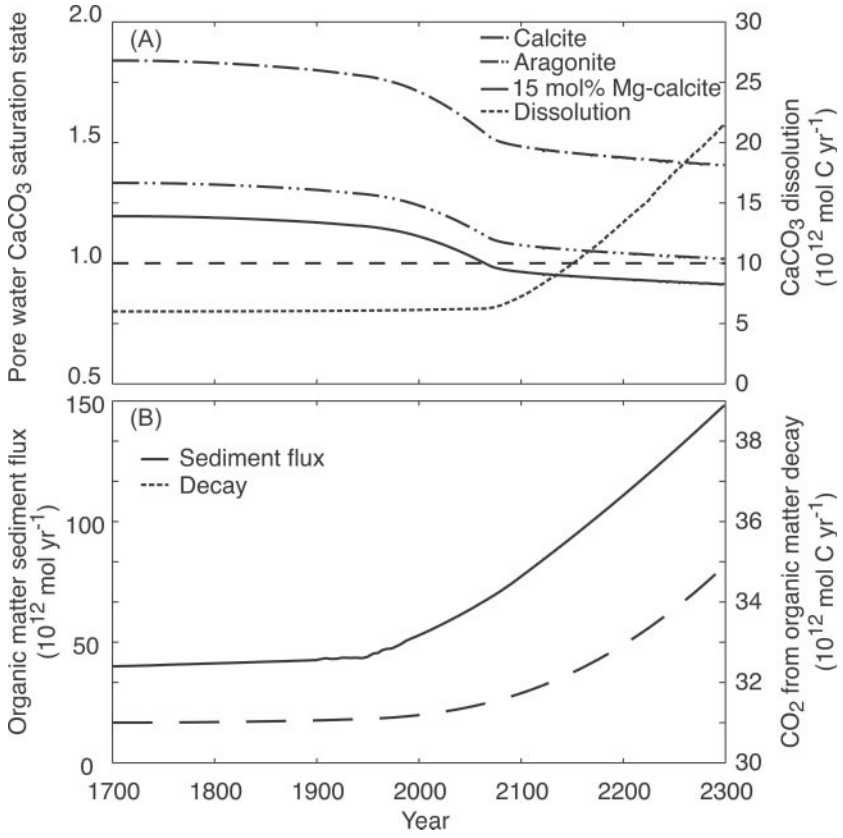

Fig. 12. (A) Pore water saturation state with respect to calcite, aragonite and 15 mol % magnesian calcite calculated at 25°C and 35 psu as well as total carbonate dissolution between the years 1700 and 2300. (B) Organic matter sediment flux and CO_2 production owing to remineralization of organic matter.

sea-to-air flux due to the decreasing flux related to the formation of carbonate minerals in the coastal ocean, and the increasingly positive difference between the terms DIC_{outflow} and DIC_{inflow} (eq 18).

Discussion of 600 years of the CO_2–carbonate system

The historical trends discussed in the preceding sections and their projection 300 years into the future would give rise to a marine CO_2-carbonic acid-carbonate system of the coastal ocean that would be considerably different from that of the recent past or the present. The most obvious outcome of the continuous rise in atmospheric CO_2 and temperature, if they were to be sustained into the future, would be a decrease in the saturation state of coastal seawater with respect to carbonate minerals. Nevertheless, the results of *SOCM* show that the surface water will remain supersaturated with respect to a magnesian calcite phase of 15 mol percent $MgCO_3$ until the final years of the simulation (fig. 11). However, it is important to realize that high latitude regions of the surface oceans will be undersaturated with respect to this phase, aragonite, and maybe also calcite much earlier than this final year (fig. 14). Although carbonate sediments are relatively rare or absent at temperate and high latitudes, calcifying organisms (mollusks, bryozoans, algae, forams, and corals) are present in abundance in these environments and may produce as much $CaCO_3$ as is produced in typical, tropical,

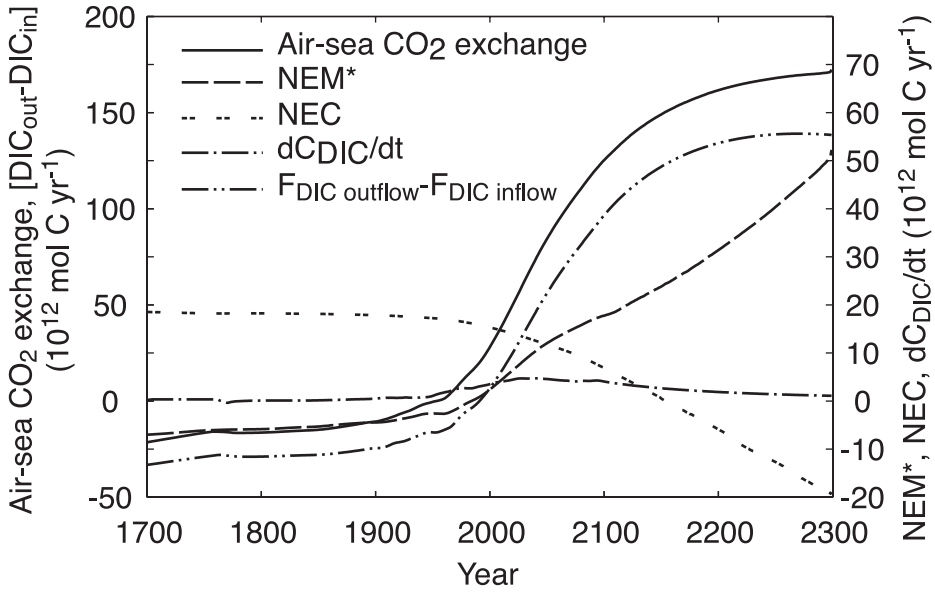

Fig. 13. Air-sea CO_2 exchange (eq 18) owing to net ecosystem metabolism (*NEM*;* eq 19), net ecosystem calcification ($CaCO_3$ precipitation less dissolution), atmospheric CO_2 concentration (dC_{DIC}/dt; eqs 15 and 18), and the imbalance of DIC between export to the open ocean and input from rivers and upwelling ($F_{DIC\ outflow} - F_{DIC\ inflow}$) between 1700 and 2300.

non-reef carbonate systems (Chave, 1967; Smith, 1972). The production of $CaCO_3$ in these high latitude and cold–water calcareous communities and realms (James, 1997) may be affected much earlier than their tropical and subtropical counterparts owing to invasion of atmospheric CO_2 (Orr and others, 2005).

The composition of modern magnesian calcite organisms, clasts, and cements in shoal–water marine calcareous environments (see the *Pore-Water-Sediment System: Carbonate Chemistry and Mineral Dissolution* sections) suggest that the seawater in which these components are immersed currently is saturated (at a metastable equilibrium) with a magnesian calcite of an approximate average composition of 12 to 15 mol percent $MgCO_3$. This is in close agreement with the carbonate saturation state of the pore water reservoir of *SOCM,* which remained close to metastable equilibrium with the adopted average sediment magnesian calcite phase of 15 mol percent once the pore water carbonate saturation state became low enough for this phase to dissolve (fig. 8). In reality, the magnesian calcite reservoir comprises a continuum of phases with different $MgCO_3$ content and mineral stability, and the average carbonate mineral composition and pore water carbonate saturation state may follow a trend similar to that of figure 8C.

The projections and calculations of seawater saturation state with respect to magnesian calcite minerals are highly dependent on the values of the experimentally derived solubility products. The solubility of magnesian calcite minerals has been a subject of substantial research, debate, and controversy (Plummer and Mackenzie, 1974; Thorstenson and Plummer, 1977, 1978; Berner, 1978; Garrels and Wollast, 1978; Lafon, 1978; Mackenzie and others, 1983; Walter and Morse, 1984; Bischoff and others, 1987, 1993; Tribble and others, 1995). One of the problems arises from the fact that a solid solution of the nature of the magnesian calcites does not attain true chemical equilibrium with an aqueous phase. According to Plummer and Mackenzie

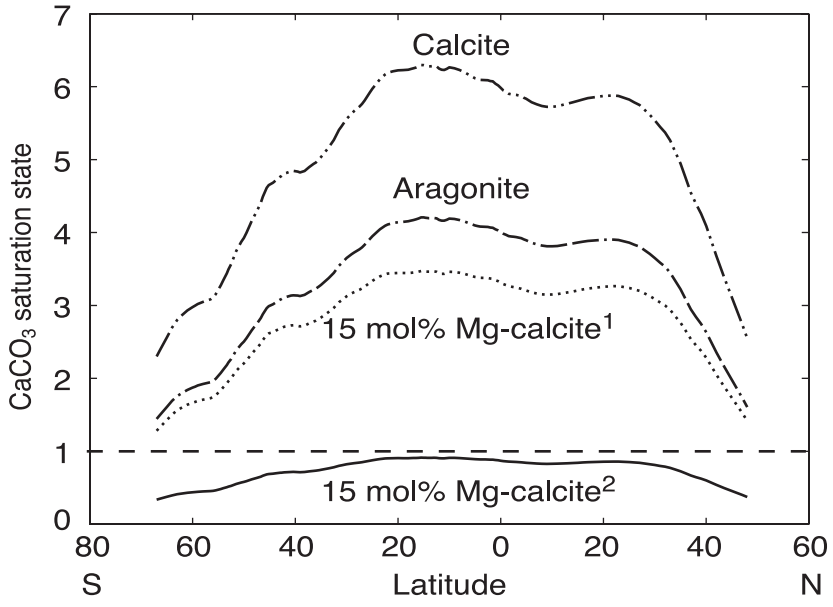

Fig. 14. Surface water saturation state with respect to calcite, aragonite, and 15 mol % magnesian calcite ([1]−log IAP = 8.18; Bischoff and others, 1987, 1993; [2]−log IAP = 7.60; Plummer and Mackenzie, 1974) as a function of latitude in the Pacific Ocean. Saturation states were calculated based on WOCE section P15 (CLIVAR and Carbon Hydrographic Data Office; http://whpo.ucsd.edu/index.htm) at *in situ* temperature and salinity following the procedure described in figure 4. Saturation state with respect to calcite and aragonite was calculated using apparent solubility constants as a function of temperature and salinity. Magnesian calcite solubility was not corrected for temperature because of the lack of data on the solubility of magnesian calcites as a function of temperature. Depending on the stoichiometric solubility product used in the calculation with respect to magnesian calcite minerals, the results are significantly different.

(1974), dissolution of a magnesian calcite phase takes place in three steps. In the first step, dissolution is a congruent process, followed by a second step of incongruent dissolution that gives rise to precipitation of a low magnesian calcite phase on original grain surfaces. Finally, during the third step, a calcium-rich phase is precipitated from the bulk solution. In order to determine the solubility of a magnesian calcite phase, solution data obtained during the congruent dissolution step are typically extrapolated to infinite time and assumed to represent equilibrium with the initial magnesian calcite composition. However, it has been pointed out that a true thermodynamic equilibrium state cannot be calculated from congruent dissolution data for the magnesian calcites, and that data extrapolated from the congruent portion of the reaction represent what is referred to as a state of stoichiometric saturation (Thorstenson and Plummer, 1977; Mackenzie and others, 1983).

In addition to the controversy associated with the concept of stoichiometric saturation, solubility results may be significantly affected by the types of pre-treatment of the biogenic magnesian calcite material being investigated (Mackenzie and others, 1983; Walter and Morse, 1984; Bischoff and others, 1987, 1993). Thus the experimentally derived stoichiometric solubility product for a specific magnesian calcite composition varies considerably between experimental studies. Nevertheless, the experimental solubility trend with composition of magnesian calcite phases has been reasonably well defined at 25°C and 1 atm pressure due to the work of Walter and Morse (1984), Bischoff and others (1987), and Busenberg and Plummer (1989), for both synthetic inorganic and biogenic phases (Tribble and others, 1995). However, considerable

uncertainty still remains concerning the dissolution and precipitation behavior of the magnesian calcites in natural environments. If a different stoichiometric solubility product for the 15 mol percent magnesian calcite were used in *SOCM* other than that obtained from the experiments of Bischoff and others (1987, 1993), the results of the model simulations and the calculated seawater saturation states with respect to magnesian calcite phases would be significantly different. To provide some feeling for this difference, we calculated the present-day latitudinal distribution of surface seawater carbonate saturation state adopting the different stoichiometric solubility products for a biogenic 15 mol percent magnesian calcite of Plummer and Mackenzie (1974) ($-\log$ IAP = 7.60) and Bischoff and others (1987, 1993) ($-\log$ IAP = 8.18) (fig. 14). Note that using the Plummer and Mackenzie value shows that seawater is very close to saturation with respect to this phase composition throughout the world's surface ocean, with the degree of slight undersaturation increasing slightly toward the colder surface waters of the higher latitudes. In addition, this calculated metastable equilibrium state is very close (within a couple of mol % $MgCO_3$) to the average composition of both magnesian calcite cements and the magnesian calcite component of shoal–water calcareous sands (Garrels and Wollast, 1978; Videtich, 1985; Agegian and Mackenzie, 1989). In contrast, using the stoichiometric solubility product for a 15 mol percent magnesian calcite as experimentally determined by Bischoff and others (1987, 1993) shows that the surface waters are highly oversaturated with respect to this phase composition.

Regardless of the above, as the saturation state of seawater declines in the future, the composition of the magnesian calcite phase in metastable equilibrium with the water will most likely decline in $MgCO_3$ content. Mackenzie and Agegian (1989) and Agegian (ms, 1985) showed that temperature, saturation state, and growth rate affected the composition of the calcareous red alga, *Porolithon gardineri,* grown in controlled microcosm experiments (fig. 15). As temperature and carbonate saturation state decreased, the extension rate of *Porolithon* also decreased as well as the magnesium content of its skeleton, where most of the variability in the magnesium content of *Porolithon* stemmed from the saturation state variable. One possible response to the lowered carbonate saturation state of coastal seawater in the future could be a decline in the magnesium content of magnesian calcite skeletal material due to both declining carbonate saturation state and lowered calcification rate. A word of caution: skeletal magnesian calcite compositions of various taxonomic groups vary as a function of latitude having less magnesium in their skeletons at the colder and more undersaturated surface waters of higher latitude (Chave 1954a, Chave, 1954b; Mackenzie and others, 1983); in addition, magnesian calcite marine cement and ooid compositions vary with latitude in much the same manner as skeletal calcite (Videtich, 1985); and furthermore, Videtich (1985) observed a strong positive correlation between decreasing temperature and magnesium content of calcite cements with increasing depth in the ocean, where both the temperature and magnesium content decrease with increasing depth. Hence both surface water carbonate saturation state and temperature potentially can affect the magnesium content of skeletal calcite organisms in the modern oceans.

It would be anticipated that as the magnesium content of various organisms with magnesian calcite skeletons changed in the future that clasts produced from their mechanical and biological disintegration would become less magnesium rich. In addition, as can be seen in figure 12, because reactive organic matter loading of coastal sediments is anticipated to increase in the future, our model simulations suggest that enhanced decomposition of organic carbon in the interstitial waters of these sediments will result in decreasing carbonate saturation state. As discussed in the *Pore Water-Sediment System: Carbonate Chemistry and Mineral Dissolution* section, magnesian calcite

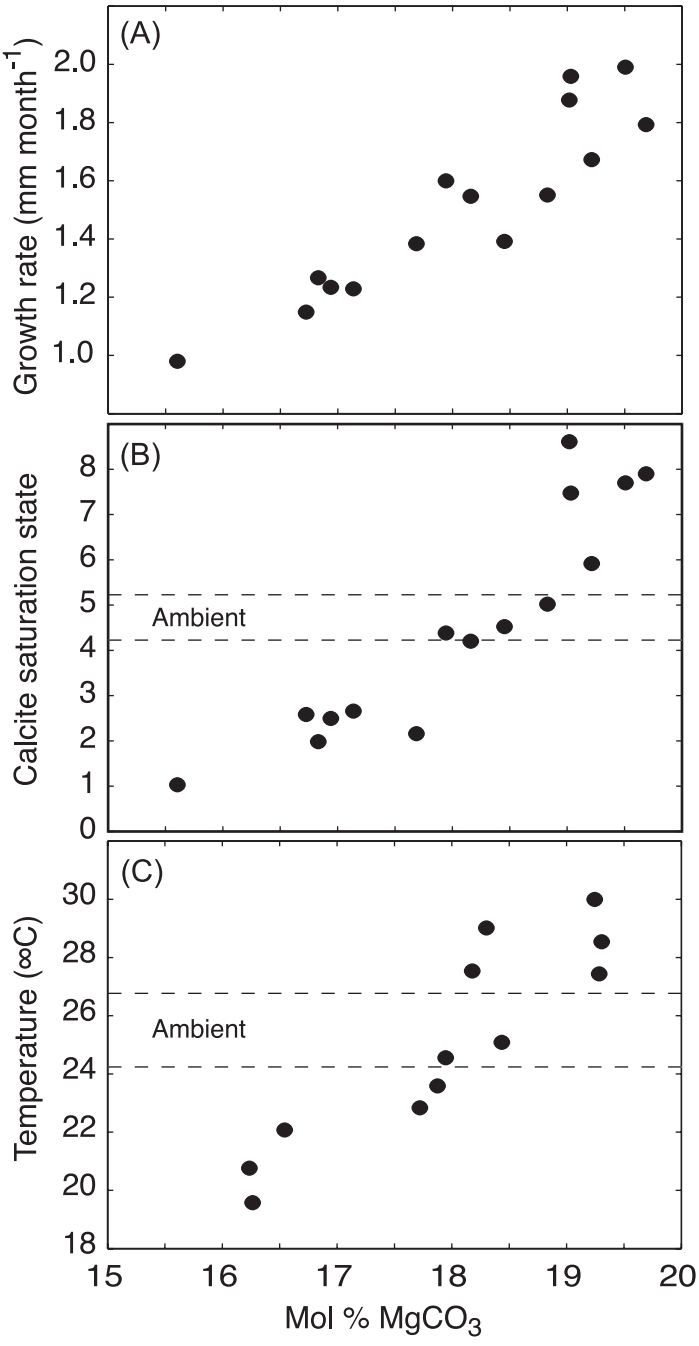

Fig. 15. Variations in mol percent $MgCO_3$ in the red coralline alga *Porolithon gardineri* as a function of (A) extension rate, (B) calcite saturation state, and (C) temperature. Adopted from Agegian (ms, 1985) and Mackenzie and Agegian (1989).

TABLE 6

Relative carbonate sediment composition in SOCM

Year	1700	2000	2300
Calcite	13%	13%	13%
Aragonite	63%	63%	66%
15 mol% Mg-calcite	24%	24%	21%

compositions that were once in metastable equilibrium with the pore water or with which the pore water was once oversaturated would have a greater tendency to dissolve. In addition, magnesian calcite cements in marine sediments would tend to have lower magnesium contents. As a result of these changes, carbonate sediment composition in the future would tend to be enriched in aragonite and calcite relative to magnesian calcite high in magnesium (table 6). Analogous to the calcite seas of the geologic past (Sandberg, 1983, 1985), several centuries into the future magnesian calcite and aragonite precipitates may become less abundant and calcites of reduced $MgCO_3$ content more abundant.

As a final thought on this matter, it is likely that the low saturation state predicted for the future might also affect the formation of carbonate ooids and whitings. The rate of formation of these carbonate deposits that are to some extent chemical precipitates from seawater depends on the saturation state of the seawater. One might anticipate that a lower saturation state might affect the rate of precipitation of these carbonate materials. Generally the lower the degree of saturation of a solution from which a carbonate phase is being precipitated, the slower the rate of precipitation, as shown, for example, in equation (10) and also discussed elsewhere (Morse and Mackenzie, 1990).

BEYOND THE YEAR 2300

Roughly at the time of the final year of the current model simulation, the atmospheric CO_2 concentration is anticipated to slowly start to decrease (Archer and others, 1998; Caldeira and Wickett, 2003). At this time, the global reservoirs of fossil fuels of approximately 5000 Gt C (Sundquist, 1985; Kvenvolden, 1988) will be very close to exhaustion and anthropogenic CO_2 emissions will have been on the decline for several decades. On a timescale of several centuries beyond our current model simulations, the ocean will absorb a substantial fraction of the anthropogenic CO_2 that has accumulated in the atmosphere (Archer and others, 1998). In part, the extent of CO_2 uptake will be dependent on the formation of deep and intermediate waters and the mixing time of the oceans, which is on the order of 1000 years. Current evidence suggests that the ocean has taken up about 48 percent of the total CO_2 emitted from burning of fossil fuels and cement manufacturing between 1800 to 1994 (see for example, Sabine and others, 2004). The uptake of anthropogenic CO_2 by the oceans will result in a shoaling of the carbonate saturation horizon in the major ocean basins, a phenomenon already being observed (Feely and others, 2004), and ultimately, also in a shoaling of the carbonate compensation depth (CCD) owing to increasing dissolution of deep sea carbonates and decreasing rain rates of biogenic carbonate hard parts produced in the surface water. According to Archer and others (1998), dissolution of deep-sea carbonate minerals will increase due to increasing CO_2 content of oceanic bottom waters, but will not play a significant role in the fate of anthropogenic CO_2 in the coming centuries. However, on a timescale of 5 to 6 ka, seafloor neutralization may account for 60 to 70 percent of anthropogenic CO_2. As the atmospheric CO_2 concentration starts to decline, the surface water ocean carbonate

saturation state most likely will start to increase. Nevertheless, the results of the present simulations clearly demonstrate that by the year 2300, coastal carbonate environments may have changed dramatically relative to today. The return toward the initial state will in part depend on the response of the open ocean to the perturbation, the residence time of global coastal waters, and the biological calcification of the shallow-ocean communities at that time.

CONCLUSIONS

The results of the numerical model simulations demonstrate that the CO_2-carbonic acid–carbonate system of the shallow–water coastal ocean would be significantly affected under future conditions of a higher CO_2 world and increased riverine transport of organic matter and nutrients to this region. The net flux of CO_2 between the surface water and the atmosphere is expected to reverse from net evasion from the coastal waters to net invasion owing to increased net ecosystem production, decreased net ecosystem calcification, and increased atmospheric CO_2 concentration from burning of fossil fuels and land-use activities. Surface water saturation state with respect to carbonate minerals (calcite, aragonite, and magnesian calcites) will decrease and consequently the rate at which calcareous organisms calcify will also decrease. It remains to be demonstrated what the ecological implications of such changes will be. It is also possible that the negative effect of decreasing carbonate saturation state could be slightly masked by other environmental variables, such as increasing temperature and DIC concentration, which indirectly may have a positive effect on the rates of biogenic calcification. Dissolution of metastable carbonate minerals will increase, but this process would not produce sufficient alkalinity (nor CO_3^{2-}) to counteract significantly any negative effects of increasing atmospheric CO_2 on a global scale nor on the timescale of several centuries. On a regional scale, a more pronounced buffer effect owing to dissolution of metastable carbonate minerals may be observed in some environments with restricted water exchange with the open ocean, such as certain atolls. The extent of carbonate dissolution in the future would be mainly controlled by transport, deposition, and decomposition of organic matter in the sediments rather than the observed changes in surface water chemistry arising from increasing atmospheric CO_2. Surface seawater of the tropics and subtropics would remain saturated even with respect to a magnesian calcite composition of 15 mol percent until the year 2300, but surface seawater at higher latitudes may be undersaturated with respect to aragonite and even calcite. However, one must be cautious when interpreting the seawater magnesian calcite saturation state because it is strongly dependent on the choice of the experimental stoichiometric solubility product that depends on the composition of the magnesian calcites. In addition, the behavior of magnesian calcite minerals in the marine environment is not well constrained. Nevertheless, the rate of formation of contemporary carbonate sediments and cements and other inorganic carbonate precipitates, such as ooids, would probably change in the future. For the magnesium-rich phases, their magnesium content is likely to decrease and carbonate sediments with lower magnesium content would become more abundant. Biogenic skeletons, shells, and tests produced by marine calcareous organisms are also likely to follow a similar trend in compositional change, as long as the external forcings of the atmospheric CO_2 increase, temperature change, and transport of nutrients and organic matter from land to the coastal ocean remain within their projected bounds.

ACKNOWLEDGMENTS

This research was supported by National Science Foundation grants ATM 00–80878, EAR 02–235090 and ATM 04–39051. Additional support was received from the Arthur L. Howland Fund of the Department of Geological Sciences, Northwestern

University. We especially thank Dr. Robert W. Buddemeier of the Kansas Geological Survey (Lawrence, Kansas) and an anonymous reviewer for their very complete and constructive reviews of the initial manuscript that led to significant improvement of the paper. This is School of Ocean and Earth Science and Technology contribution no. 6704.

References

Agegian, C. R., ms, 1985, The biogeochemical ecology of *Porolithon gardineri* (foslie): Ph.D. thesis, University of Hawaii, Honolulu, 178 p.

Agegian, C. R., and Mackenzie, F. T., 1989. Calcareous organisms and sediment mineralogy on a mid-depth bank in the Hawaiian archipelago: Pacific Science, v. 43, p. 56–66.

Andersson, A. J., ms, 2003, Climate change and anthropogenic effects on shallow-water carbonate biogeochemistry: M.S. thesis, University of Hawaii, Honolulu, 195 p.

Andersson, A. J., and Mackenzie, F. T., 2004, The shallow-water ocean: a source or sink of atmospheric CO_2?: Frontiers in Ecology and the Environment, v. 2, p. 348–353.

Andersson, A. J., Mackenzie, F. T., and Ver, L. M., 2003, Solution of shallow-water carbonates: An insignificant buffer against rising atmospheric CO_2: Geology, v. 31, p. 513–516.

Archer, D., Kheshgi, H., and Maier-Reimer, E., 1998, Dynamics of fossil fuel CO_2 neutralization by marine $CaCO_3$: Global Biogeochemical Cycles, v. 12, p. 259–276.

Bacastow, R. D., and Keeling, C. D., 1973, Atmospheric carbon dioxide and radiocarbon in the natural carbon cycle: II. Changes from A.D. 1700 to 2070 as deduced from a geochemical model, *in* Woodwell, G. M., and Pecan, E. V., editors, Carbon and the Biosphere: United States Atomic Energy Commission, p. 86–135.

Balzer, W., and Wefer, G., 1981, Dissolution of carbonate minerals in a subtropical shallow marine environment: Marine Chemistry, v. 10, p. 545–558.

Barnes, D. J., and Cuff, C., 2000, Solution of reef rock buffers seawater against rising atmospheric CO_2, *in* Hopley, D., Hopley, M., Tamelander, J., and Done, T., editors, Proceedings of the Ninth International Coral Reef Symposium Abstracts: State Ministry for the Environment, Indonesia, p. 248.

Barnola, J. M., Anklin, M., Procheron, J., Reynaud, D., Schwander, D., and Stauffer, B., 1995, CO_2 evolution during the last millenium as recorded by Antarctic and Greenland ice: Tellus, v. 47B, p. 264–272.

Bates, N. R., 2001, Interannual variability of oceanic CO_2 and biogeochemical properties in the Western North Atlantic subtropical gyre: Deep-Sea Research II, v. 48, p. 1507–1528.

Bates, N. R., Michaels, A. F., and Knap, A. H., 1996, Seasonal and interannual variability of the oceanic carbon dioxide system at the U.S. JGOFS Bermuda Atlantic Time-series site: Deep-Sea Research II, v. 43, p. 347–383.

Berner, R. A., 1978, Equilibrium kinetics, and the precipitation of magnesian calcite from seawater: American Journal of Science, v. 276, p. 713–730.

Berner, R. A., Westrich, J. T., Graber, R., Smith, J., and Martens, C. S., 1978, Inhibition of aragonite precipitation from supersaturated seawater: A laboratory and field study: American Journal of Science, v. 278, p. 816–837.

Bessat, F., and Buiges, A. D., 2001, Two centuries of variation in coral growth in a massive *Porites* colony from Moorea (French Polynesia): A response of ocean-atmosphere variability from south central Pacific: Paleogeography, Paleoclimatology, Paleoecology, v. 175, p. 381–392.

Bijma, J., Spero, H. J., and Lea, D. W., 1999, Reassessing foraminiferal stable isotope geochemistry: Impacts of the oceanic carbonate system (experimental results), *in* Fisher, G., and Wefer, G., editors, Use of Proxies in Paleoceanography: Example from the South Atlantic: New York, Springer-Verlag, p. 489–512.

Bijma, J., Hönisch, B., and Zeebe, R. E., 2002, Impact of the ocean carbonate chemistry on living foraminiferal shell weight: Comment on "Carbonate ion concentration in glacial-age deep waters of the Caribbean Sea" by W. S. Broecker and E. Clark: Geochemistry, Geophysics, Geosystems, v. 3(11), 1064, doi:10.1029/2002GC000388.

Bischoff, W. D., Mackenzie, F. T., and Bishop, F. C., 1987, Stabilities of synthetic magnesian calcites in aqueous solution: comparison with biogenic materials: Geochimica et Cosmochimica Acta, v. 51, p. 1413–1423.

Bischoff, W. D., Bertram, M. A., Mackenzie, F. T., and Bishop, F. C., 1993, Diagenetic stabilization pathways of magnesian calcites: Carbonates and Evaporites, v. 8, p. 82–89.

Borges, A., 2005, Do we have enough pieces of the jigsaw to integrate CO_2 fluxes in the coastal ocean: Estuaries, v. 26, p. 3–27.

Borowitzka, M. A., 1981, Photosynthesis and calcification in the articulates coralline red algae *Amphiroa anceps* and *A. foliacea*: Marine Biology, v. 62, p. 17–23.

Boucher, G., Clavier, J., Hily, C., and Gattuso, J. P., 1998, Contribution of soft-bottoms to the community metabolism (primary production and calcification) of a barrier reef flat (Moorea, French Polynesia): Journal of Experimental Marine Biology and Ecology, v. 225, p. 269–283.

Buddemeier, R. W., Kleypas, J. A., and Aronson, R. B., 2004, Coral reefs and global climate change: Potential contributions of climate change to stresses on coral reef ecosystems: Report prepared for the Pew Center on Global Climate Change, Arlington, Virginia, 44 p.

Busenberg, E., and Plummer, N. L., 1989, Thermodynamics of magnesian calcite solid solution-solutions at 25°C and 1 atm total pressure: Geochimica et Cosmochimca Acta, v. 53, p. 1189–1208.

Caldeira, K., and Wickett, M. E., 2003, Anthropogenic carbon and ocean pH: Nature, v. 425, p. 365.
Chave, K. E., 1954a, Aspects of the biogeochemistry of magnesium 1. Calcareous sediments and rocks: The Journal of Geology, v. 62, p. 266–283.
——— 1954b, Aspects of the biogeochemistry of magnesium 2. Calcareous sediments and rocks: The Journal of Geology, v. 62, p. 587–599.
——— 1962, Factors influencing the mineralogy of carbonate sediments: Limnology and Oceanography, v. 7, p. 218-223.
——— 1967, Recent carbonate sediments: An unconventional view: Journal of Geological Education, v. 15, p. 200–204.
Chavez, F. P., and Toggweiler, J. R., 1995, Physical estimates of global new production: The upwelling contribution, *in* Summerhayes, C. P., Emeis, K. C., Angel, M. V., Smith, R. L., and Zeitzschel, B., editors, Upwelling in the ocean: Modern processes and ancient records: England, John Wiley and Sons, p. 313–320.
Chen, C. T. A., Rodman, M. R., Wei, C. L., Olson, E. J., Feely, R. A., and Gendron, J. F., 1986, Carbonate chemistry of the North Pacific Ocean: Washington, D. C., United States Department of Energy, 176 p.
Clausen, C. D., and Roth, A. A., 1975, Effect of temperature and temperature adaptation on calcification rate in the hermatypic coral *Pocillopora damicornis*: Marine Biology, v. 33, p. 93–100.
Cohen, A. L., and McConnaughey, T. A., 2003, Geochemical perspectives on coral mineralization, *in* Dove, P. M., De Yoreo, J. J., and Weiner, S., editors, Biomineralization: Mineralogical Society of America, Reviews in Mineralogy and Geochemistry, v. 54, p. 151–187.
Delesalle, B., and Sournia, A., 1992, Residence time of water and phytoplankton biomass in coral reef lagoons: Continental Shelf Research, v. 12, p. 939–949.
Dickson, A., and Millero, F. J., 1987, A comparison of the equilibrium constants for the dissociation of carbonic acid in seawater media: Deep-Sea Research, v. 38, p. 1733–1743.
Dubus, I. G., and Brown, C. D., 2002, Organic compounds in the environment: sensitivity and first-step uncertainty analyses for the preferential flow model MACRO: Journal of Environmental Quality, v. 31, p. 227–240.
Enting, I. G., Wigley, T. M. L., and Heimann, M., 1995, Intergovernmental Panel on Climate Change (IPCC), Working Group 1, 1994: Modelling Results Relating Future Atmospheric CO_2 Concentrations to Industrial Emissions: Oak Ridge, Tennessee, U.S.A., U.S. Department of Energy, Oak Ridge National Laboratory, ORNL/CDIAC DB1009, Carbon Dioxide Information Analysis Center.
Etheridge, D. M., Steele, L. P., Langenfelds, R. L., Francey, R. J., Barnola, J. M., and Morgan, V. I., 1996, Natural and anthropogenic changes in atmospheric CO_2 over the last 1000 years from air in Antarctic ice and firn: Journal of Geophysical Research, v. 101, p. 4115–4128.
Feely, R. A., Sabine, C. L., Lee, K., Berelson, W., Kleypas, J., Fabry, V. J., and Millero, F. J., 2004, Impact of anthropogenic CO_2 on the $CaCO_3$ system in the oceans: Science, v. 305, p. 362–366.
Ferrier-Pages, C., Gattuso, J. P., Dallot, S., and Jaubert, J., 2000, Effect of nutrient enrichment on growth and photosynthesis of the zooxanthellate coral *Stylophora pistillata:* Coral Reefs, v. 19, p. 103–113.
Frankignoulle, M., Canon, C., and Gattuso, J. P., 1994, Marine calcification as a source of carbon dioxide: Positive feedback of increasing atmospheric CO_2: Limnology and Oceanography, v. 39, p. 458–462.
Friedli, H., Lotscher, H., Oeschger, H., Siegenthaler, U., and Stauffer, B., 1986, Ice core record of the $^{13}C/^{12}C$ ratio of atmospheric carbon dioxide in the past two centuries: Nature, v. 324, p. 237–238.
Gao, K., Aruga, Y., Asada, K., Ishihara, T., Akano, T., and Kiyohara, M., 1993, Calcification in the articulated coralline alga *Coralline pilulifera,* with special reference to the effect of elevated CO_2 concentration: Marine Biology, v. 117, p. 129–132.
Gardner, T. A., Côté, I. M., Gill, J. A., Grant, A., and Watkinson, A. R., 2003, Long-term region-wide declines in Caribbean corals: Science, v. 301, p. 958–960.
Garrels, R. M., and Mackenzie, F. T., editors, 1980, Some aspects of the role of the shallow ocean in global carbon dioxide uptake, Workshop report: United States Department of Energy, Carbon dioxide effects research and assessment program.
Garrels, R., and Wollast, R., 1978, Equilibrium criteria for two-component solids reacting with fixed composition in an aqueous phase—Example: the magnesian calcite, Discussion: American Journal of Science, v. 278, p. 1469–1474.
Gattuso, J. P., Frankignoulle, M., Bourge, I., Romaine, S., and Buddemeier, R. W., 1998, Effect of calcium carbonate saturation of seawater on coral calcification: Global Planetary Change, v. 18, p. 37–46.
Gattuso, J. P., Allemand, P. D., and Frankignoulle, M., 1999, Interactions between the carbon and carbonate cycles at organism and community levels on coral reefs: A review of processes and control by carbonate chemistry: American Zoologist, v. 39, p. 160–188.
Grigg, R. W., 1982, Coral reef development at high latitudes in Hawaii, *in* Gomez, E. D., Birkeland, C. E., Buddemeier, R. W., Johannes, R. E., Marsh, J.A., Jr., and Tsuda, R. T., editors, Proceedings of the Fourth International Coral Reef Symposium: Manila, Philippines, University of the Philippines, Marine Sciences Center, v. 1, p. 687–693.
——— 1997, Paleoceanography of coral reefs in the Hawaiian-Emperor Chain—revisited: Coral Reefs, v. 16, p. S33–S38.
Halley, R. B., and Yates, K. K., 2000, Will reef sediments buffer corals from increased global CO_2, *in* Hopley, D., Hopley, M., Tamelander, J., and Done, T., editors, Proceedings of the Ninth International Coral Reef Symposium Abstracts: Indonesia, State Ministry for the Environment, p. 248.
Hamby, D. M., 1994, A review of techniques for parameter sensitivity analysis of environmental models: Environmental Monitoring and Assessment, v. 32, p. 135–151.
Hawaiian Ocean Time series (HOTs), 2004, *http://hahana.soest.hawaii.edu/hot/hot_jgofs.html*

Houghton, J. T., Meiro Filho, L. G., Callander, B. A., Harris, N., Kattenberg, A., and Maskell, K., editors, 1996, Climate change 1995: The science of climate change, Contribution of working group I to the Second Assessment Report of the intergovernmental Panel on Climate Change: Cambridge, Cambridge University Press, 572 p.

Houghton, J. T., Ding, Y., Griggs, D. J., Noguer, M., van der Linden, P. J., Dai, X., Maskell, K., and Johnson, C. A., editors, 2001, Climate change 2001: The scientific basis, Contribution of Working Group I to the Third Assessment Report of the Intergovernmental Panel on Climate Change: Cambridge, Cambridge University Press, 881 p.

Hutchings, P. A., 1986, Biological destruction of coral reefs: Coral Reefs, v. 4, p. 239–252.

James, N. P., 1997, The cool-water carbonate depositional realm, *in* James, N. P., and Clarke, J. A. D., editors, Cool-water carbonates: Tulsa, Oklahoma, Society for Sedimentary Geology, Special Publication No. 56, p. 1–20.

Keeling, C. D., and Whorf, T. P., 2002, Atmospheric CO_2 records from sites in the SIO air sampling network, *in* Trends: A Compendium of Data on Global Change: Oak Ridge, Tennessee, U. S. A., Oak Ridge National Laboratory, Carbon Dioxide Information Analysis Center, United States Department of Energy.

Keeling, C. D., Chin, J. F. S., and Whorf, T. P., 1996, Increased activity of northern vegetation inferred from atmospheric CO_2 measurements: Nature, v. 382, p. 146–149.

Kleypas, J. A., Buddemeier, R. W., Archer, D., Gattuso, J. P., Langdon, C., and Opdyke, B. N., 1999, Geochemical consequences of increased atmospheric carbon dioxide on coral reefs: Science, v. 284, p. 118–120.

Kleypas, J. A., Buddemeier, R. W., and Gattuso, J. P., 2001, The future of coral reefs in an age of global change: International Journal of Earth Sciences (Geologische Rundschau), v. 90, p. 426–437.

Kleypas, J. A., Buddemeier, R. W., Eakin, C. M., Gattuso, J. P., Guinotte, J., Hoegh-Guldberg, O., Iglesias-Prieto, R., Jokiel, P. L., Langdon, C., Skirving, W., and Strong, A. E., 2005, Comment on "Coral reef calcification and climate change: The effect of ocean warming": Geophysical Research Letters, v. 32, doi:10.1029/2004GL022329.

Kvenvolden, K. A., 1988, Methane—a major reservoir of carbon on a shallow geosphere?: Chemical Geology, v. 71, p. 41–51.

Lafon, G. M., 1978, Equilibrium criteria for two-component solids reacting with fixed composition in an aqueous phase-example: the magnesian calcites: American Journal of Science, v. 278, p. 1455–1468.

Langdon, C., 2002, Review of experimental evidence for effects of CO_2 on calcification of reef builders, *in* Kasim Moosa, M. K., Soemodihardjo, S., Nontji, A., Soegiarto, A., Romimohtarto, K., Sukarno, and Suharsono, editors, Proceedings of the 9th International Coral Reef Symposium: Ministry of Environment, the Indonesian Institute of Sciences and the International Society for Reef Studies, v. 2, p. 1091–1098.

Langdon, C., Takahashi, T., Sweeney, C., Chipman, D., Goddard, J., Marubini, F., Aceves, H., Barnett, H., and Atkinson, M., 2000, Effect of calcium carbonate saturation state on the calcification rate of an experimental coral reef: Global Biogeochemical Cycles, v. 14, p. 639–654.

Langdon, C., Broecker, W. S., Hammond, D. E., Glenn, E., Fitzsimmons, K., Nelson, S. G., Peng, T. H., Hajdas, I., and Bonani, G., 2003, Effect of elevated CO_2 on the community metabolism of an experimental coral reef: Global Biogeochemical Cycles, v. 17, doi:10.1029/2002GB001941.

Leclercq, N., Gattuso, J. P., and Jaubert, J., 2000, CO_2 partial pressure controls the calcification rate of a coral community: Global Change Biology, v. 6, p. 329–334.

——— 2002, Primary production, respiration, and calcification of a coral reef mesocosm under increased CO_2 partial pressure: Limnology and Oceanography, v. 47, p. 558–564.

Lerman, A., and Mackenzie, F. T., 2004, CO_2 air-sea exchange due to calcium carbonate and organic matter storage: pre-industrial and Last Glacial Maximum estimates: Biogeosciences Discussions, v. 1, p. 429–495.

——— 2005, CO_2 air-sea exchange due to calcium carbonate and organic matter storage, and its implications for the global carbon cycle: Aquatic Geochemistry, v. 11, p. 345–390, DOI: 10.1007/S10498-005-8620-X.

Lerman, A., Mackenzie, F. T., and Ver, L. M., 2004, Coupling of the perturbed C-N-P cycles in industrial time: Aquatic Geochemistry, v. 10, p. 3–32.

Lewis, E., and Wallace, D. W. R., 1998, Program Developed for CO_2 System Calculations, ORNL/CDIAC-105: Oak Ridge, Tennessee, Carbon Dioxide Information Analysis Center, Oak Ridge National Laboratory, United States Department of Energy.

Lough, J. M., and Barnes, D. J., 2000, Environmental control on the massive coral *Porites:* Journal of Experimental Marine Biology and Ecology, v. 245, p. 225–243.

Mackenzie, F. T., 2003, Our Changing Planet: An Introduction to Earth System Science and Global Environmental Change: Upper Saddle River, New Jersey, Prentice-Hall, 580 p.

Mackenzie, F. T., and Agegian, C. R., 1989, Biomineralization and tentative links to plate tectonics, *in* Crick, R. E., editor, Origin, evolution, and modern aspects of biomineralization in plants and animals: New York, Plenum Press, p. 11–27.

Mackenzie, F. T., Bischoff, W. D., Bishop, F. C., Loijens, M., Schoonmaker, J., and Wollast, R., 1983, Magnesian calcites: Low temperature occurrence, solubility and solid-solution behavior, *in* Reeder, R. J., editor, Carbonates: Mineralogy and Chemistry: Mineralogical Society of America, Reviews in Mineralogy, v. 11, p. 97–143.

Mackenzie, F. T., Lerman, A., and Ver, L. M., 1998, Role of the continental margin in the global carbon balance during the past three centuries: Geology, v. 26, p. 423–426.

Mackenzie, F. T., Ver, L. M., and Lerman, A., 2000, Coastal-zone biogeochemical dynamics under global warming: International Geology Review, v. 42, p. 193–206.

——— 2002, Century-scale nitrogen and phosphorus controls of the carbon cycle: Chemical Geology, v. 190, p. 13–32.
Mackenzie, F. T., Lerman, A., and Andersson, A. J., 2004a, Past and present of sediment and carbon biogeochemical cycling models: Biogeosciences, v. 1, p. 11–32.
Mackenzie, F. T., Andersson, A. J., Lerman, A., and Ver, L. M., 2004b, Boundary exchanges in the global coastal margin: implications for the organic and inorganic carbon cycles, *in* Robinson, A. R., McCarthy, J., and Rothschild, B. J., editors, The Sea: Cambridge, Massachusetts, Harvard University Press, v. 13, p. 193–225,
Marshall, A. T., and Clode, P., 2004, Calcification rate and the effect of temperature in a zooxanthellate and an azooxanthellate scleractinian reef coral: Coral reefs, v. 23, p. 218–224.
Marubini, F., and Atkinson, M. J., 1999, Effects of lowered pH and elevated nitrate on coral calcification: Marine Ecology Progress Series, v. 188, p. 117–121.
Marubini, F., and Thake, B., 1999, Bicarbonate addition promotes coral growth: Limnology and Oceanography, v. 44, p. 716–720.
Marubini, F., Barnett, H., Langdon, C., and Atkinson, M. J., 2001, Dependence of calcification on light and carbonate ion concentration for the hermatypic coral *Porites compressa:* Marine Ecology Progress Series, v. 220, p. 153–162.
Marubini, F., Ferrier-Pagés, C., and Cuif, J. P., 2003, Suppression of skeletal growth in scleractinian corals by decreasing ambient carbonate-ion concentration: a cross-family comparison: Proceedings of the Royal Society of London: Series B: Biological Sciences, v. 270, p. 179–184.
McConnaughey, T. A., and Whelan, J. F., 1997, Calcification generates protons for nutrient and bicarbonate uptake: Earth-Science Reviews, v. 42, p. 95–117.
McConnaughey, T. A., Adey, W. H., and Small, A. M., 2000, Community and environmental influences on reef coral calcification: Limnology and Oceanography, v. 45, p. 1667–1671.
McNeil, B. I., Matear, R. J., and Barnes, D. J., 2004, Coral reef calcification and climate change: the effect of ocean warming: Geophysical Research Letters, v. 31, L22309, doi:10.1029/2004GL021541.
Mehrbach, C., Culberson, C. H., Hawley, J. E., and Pytkowicz, R. M., 1973, Measurement of the apparent dissociation constants of carbonic acid in seawater at atmospheric pressure: Limnology and Oceanography, v. 18, p. 897–907.
Meybeck, M., 1982, Carbon, nitrogen, and phosphorus transport by world rivers: American Journal of Science, v. 282, p. 401–450.
——— 2001, Global alteration of riverine geochemistry under human pressure, *in* Ehlers, E., and Krafft, T., editors, Understanding the Earth System: Compartments, Processes, and Interactions: Heidelberg, Germany, Springer, p. 97–113.
Meybeck, M., and Ragu, A., 1995, River discharges to the oceans: An assessment of suspended solids, major ions and nutrients: Nairobi, Kenya, United Nations Environment Programme, Report, 245 p.
——— 1997, Presenting GEMS GLORI: A compendium of world river discharges to the oceans, *in* Webb, B., editor, Freshwater Contamination, Proceedings of a symposium held during the Fifth IAHS Scientific Assembly at Rabat, April–May 1997: International Association of Hydrological Sciences, v. 243, p. 3–14.
Millero, F. J., and Pierrot, D., 1998, A chemical equilibrium model for natural waters: Aquatic Geochemistry, v. 4, p. 153–199.
Milliman, J. D., 1974, Recent sedimentary carbonates, Part 1: Marine carbonates: Berlin, Springer-Verlag, 375 p.
——— 1993, Production and accumulation of calcium carbonate in the ocean: Budget of a nonsteady state: Global Biogeochemical Cycles, v. 7, p. 927–957.
Milliman, J. D., and Droxler, A. W., 1996, Neritic and pelagic carbonate sedimentation in the marine environment: ignorance is not bliss: Geologische Rundschau, v. 85, p. 496–504.
Milliman, J. D., Troy, P. J., Balch, W. M., Adams, A. K., Li, Y. H., and Mackenzie, F. T., 1999, Biologically mediated dissolution of calcium carbonate above the chemical lysocline?: Deep-Sea Research I, v. 46, p. 1653–1669.
Morse, J. W., 1983, The kinetics of calcium carbonate dissolution and precipitation, *in* Reeder, R. J., editor, Carbonates: Mineralogy and Chemistry: Mineralogical Society of America, Reviews in Mineralogy, v. 11, p. 227–264.
Morse, J. W., and Mackenzie, F. T., 1990, Geochemistry of Sedimentary Carbonates: Amsterdam, Elsevier Science Publishing Company, 707 p.
Morse, J. W., Zullig, J. J., Bernstein, L. D., Millero, F. J., Milne, P., Mucci, A., and Choppin, G. R., 1985, Chemistry of calcium carbonate-rich shallow water sediments in the Bahamas: American Journal of Science, v. 285, p. 147–185.
Moulin, E., Jordens, A., and Wollast, R., 1985, Influence of the aerobic bacterial respiration on the early dissolution of carbonates in coastal sediments: Brussels, Belgium, Proceedings Progress in Belgium Oceanographic Research, p. 196–208.
Neftel, A., Moor, E., Oeschger, H., Turekian, K. K., and Dodge, R. E., 1985, Evidence from polar ice cores for the increase in atmospheric CO_2 in the past two centuries: Nature, v. 315, p. 45–47.
Neumann, A. C., 1965, Processes of recent carbonate sedimentation in Harrington sound Bermuda: Bulletin of Marine Science, v. 15, p. 987–1035.
Ohde, S., and van Woesik, R., 1999, Carbon dioxide flux and metabolic processes of a coral reef, Okinawa: Bulletin of Marine Science, v. 65, p. 559–576.
Orr, J. C., Fabry, V. J., Aumont, O., Bopp, L., Doney, S. C., Feely, R. A., Gnanadesikan, A., Gruber, N., Ishida, A., Joos, F., Key, R. M., Lindsay, K., Maier-Reimer, E., Matear, R., Monfray, P., Mouchet, A., Najjar, R. G., Plattner, G. K., Rodgers, K. B., Sabine, C. L., Sarmiento, J. L., Schlitzer, R., Slater, R. D., Totterdell, I. J., Weirig, M. F., Yamanaka, Y., and Yool, A., 2005, Anthropogenic ocean acidification over the twenty-first century and its impacts on calcifying organisms: Nature, v. 437, p. 681–686.

Paasche, E., and Brubak, S., 1994, Enhanced calcification in the coccolithophorid *Emiliania huxleyi* (Haptophyceae) under phosphorus limitation: Phycologia, v. 33, p. 324–330.
Plummer, L. N., and Busenberg, E., 1982, The solubilities of calcite, aragonite and vaterite in CO_2-H_2O solutions between 0-90°C and an evaluation of the aqueous model for the system $CaCO_3$-CO_2-H_2O: Geochimica et Cosmochimica Acta, v. 46, p. 1011–1040.
Plummer, L. N., and Mackenzie, F. T., 1974, Predicting mineral solubility from rate data: application to the dissolution of magnesian calcites: American Journal of Science, v. 274, p. 61–83.
Raven, J. A., 1993, Limits on growth rates: Nature, v. 361, p. 209–210.
——— 1997, Inorganic carbon acquisition by marine autotrophs: Advances of Botanical Research, v. 27, p. 85–209.
Revelle, R., and Munk, W., 1977, The carbon dioxide cycle and the biosphere, *in* N. G. S. Committee, editors, Energy and Climate: Washington, D. C., National Academy Press, p. 140–158.
Reynaud, S., Leclercq, N., Romaine-Lioud, S., Ferrier-Pagés, C., Jaubert, J., and Gattuso, J. P., 2003, Interacting effects of CO_2 partial pressure and temperature on photosynthesis and calcification in a scleractinian coral: Global Change Biology, v. 9, p. 1660–1668, doi: 10.1046/j.1529-8817.2003.00678.x.
Riebesell, U., Wolf-Gladrow, D., and Smetack, V., 1993, Carbon dioxide limitation of phytoplankton growth rates: Nature, v. 361, p. 249–251.
Riebesell, U., Zondervan, I., Rost, B., Tortell, P. D., Zeebe, R. E., and Morel, F. M. M., 2000, Reduced calcification of marine plankton in response to increased atmospheric CO_2: Nature, v. 407, p. 364–367.
Sabine, C. L., Feely, R. A., Gruber, N., Key, R. M., Lee, K., Bullister, J. L., Wanninkhof, R., Wong, C. S., Wallace, D. W. R., Tilbrook, B., Millero, F. J., Peng, T. H., Kozyr, A., Ono, T., and Rios, A. F., 2004, The oceanic sink for anthropogenic CO_2: Science, v. 305, p. 367–371.
Sandberg, P. A., 1983, An oscillating trend in Phanerozoic non-skeletal carbonate mineralogy: Nature, v. 305, p. 19–22.
——— 1985, Nonskeletal aragonite and pCO_2 in the Phanerozoic and Proterozoic, *in* Sundquist, E. T., and Broecker, W. S., editors, The Carbon Cycle and Atmospheric CO_2: Natural Variations Archean to Present: Washington, D. C., American Geophysical Union, Geophysical Monograph Series, v. 32, p. 585–594.
Sarmiento, J. L., and Gruber, N., 2002, Sinks for anthropogenic carbon: Physics Today, v. 55, p. 30–36.
Sarmiento, J. L., and Sundquist, E. T., 1992, Revised budget for the oceanic uptake of anthropogenic carbon dioxide: Nature, v. 356, p. 589–593.
Schmalz, R. F., and Chave, K. E., 1963, Calcium carbonate: Affecting saturation in ocean waters of Bermuda: Science, v. 139, p. 1206–1207.
Sciandra, A., Harlay, J., Lefèvre, D., Lemée, R., Rimmelin, P., Denis, M., and Gattuso, J. P., 2003, Response of coccolithophorid Emiliania huxleyi to elevated partial pressure of CO_2 under nitrogen limitation: Marine Ecology Progress Series, v. 261, p. 111–122.
Scoffin, T. P., Tudhope, A. W., Brown, B. E., Chansang, H., and Cheeney, R. F., 1992, Patterns and possible environmental controls of skeletogenesis of Porites lutea, South Thailand: Coral Reefs, v. 11, p. 1–11.
Smith, A. D., and Roth, A. A., 1979, Effect of carbon dioxide concentration on calcification in the red coralline alga *Bossiella orbigniana*: Marine Biology, v. 52, p. 217–225.
Smith, S. V., 1972, Production of calcium carbonate on the mainland shelf of southern California: Limnology and Oceanography, v. 17, p. 28–41.
——— 1978, Coral-reef area and the contribution of reefs to processes and resources of the world's oceans: Nature, v. 273, p. 225–226.
——— 1985, Physical, chemical and biological characteristics of CO_2 gas flux across the air-water interface: Plant Cell and Environment, v. 8, p. 387–398.
Smith, S. V., and Hollibaugh, J. T., 1993, Coastal metabolism and the oceanic organic carbon balance: Reviews of Geophysics, v. 31, p. 75–89.
Smith, S. V., and Mackenzie, F. T., 1987, The ocean as a net heterotrophic system: Implications from the carbon biogeochemical cycle: Global Biogeochemical Cycles, v. 1, p. 187–198.
Spero, H. J., Bijma, J., Lea, D. W., and Bemis, B. E., 1997, Effect of seawater carbonate concentration on foraminiferal carbon and oxygen isotopes: Nature, v. 390, p. 497–500.
Sundquist, E. T., 1985, Geological perspectives on carbon dioxide and the carbon cycle, *in* Sundquist, E. T., and Broecker, W. S., editors, The Carbon Cycle and Atmospheric CO_2: Natural Variations Archean to Present: Washington, D. C., American Geophysical Union, Geophysical Monograph Series 32, p. 5–59.
Takahashi, T., Broecker, W. S., Brainbridge, A. E., and Weiss, R. F., 1980, Carbonate chemistry of the Atlantic, Pacific and Indian Oceans: The results of the GEOSECS expeditions, 1972–1978, Technical Report No. 1, CV-1-80: Palisades, New York, Lamont-Doherty Geological Observatory.
Thorstenson, D. C., and Mackenzie, F. T., 1974, Time variability of pore water chemistry in recent carbonate sediments, Devil's Hole, Harrington Sound, Bermuda: Geochimica et Cosmochimica Acta, v. 38, p. 1–19.
Thorstenson, D. C., and Plummer, L. N., 1977, Equilibrium criteria for two component solids reacting with fixed composition in an aqueous phase-example: the magnesian calcites: American Journal of Science, v. 277, p. 1203–1223.
——— 1978, Equilibrium criteria for two component solids reacting with fixed composition in an aqueous phase-example: the magnesian calcites, reply: American Journal of Science, v. 278, p. 1478–1488.
Tribble, J. S., Arvidson, R. S., Lane III, M., and Mackenzie, F. T., 1995, Crystal chemistry, and thermodynamic and kinetic properties of calcite, dolomite, apatite, and biogenic silica: applications to petrological problems: Sedimentary Geology, v. 95, p. 11–37.

Ver, L. M. B., ms, 1998, Global kinetic models of the coupled C, N, P, and S biogeochemical cycles: implications for global environmental change: Honolulu, University of Hawaii, Ph.D. thesis, xxii + 681 p.
Ver, L. M., Mackenzie, F. T., and Lerman, A., 1994, Modeling pre-industrial C-N-P-S biogeochemical cycling in the land-coastal margin system: Chemosphere, v. 29, p. 855–887.
——— 1998, Partitioning of anthropogenic CO_2 by C-N-P-S cycle coupling on land and in coastal oceanic environment: Mineralogical Magazine, v. 62A, p. 1589–1590.
——— 1999a, Biogeochemical responses of the carbon cycle to natural and human perturbations: Past, present, and future: American Journal of Science, v. 299, p. 762–801.
——— 1999b, Carbon cycle in the coastal zone: Effects of global perturbations and change in the past three centuries: Chemical Geology, v. 159, p. 283–304.
Videtich, P. E., 1985, Electron microprobe study of Mg distribution in recent Mg calcites and recrystallized equivalents from the Pleistocene and Tertiary: Journal of Sedimentary Petrology, v. 55, p. 421–429.
Voluer, M., ms, 2004, Dissolution of metastable carbonate minerals: effects of physical mixing and potential as a buffer against rising atmospheric CO_2 in coral reef ecosystems: Honolulu, Hawaii, University of Hawaii, Honolulu, B.S. thesis, 63 p.
Walter, L. M., and Morse, J. W., 1984, Reactive surface area of skeletal carbonate during dissolution: Effect of grain size: Journal of Sedimentary Petrology, v. 54, p. 1081–1090.
——— 1985, The dissolution kinetics of shallow marine carbonates in seawater: A laboratory study: Geochimica et Cosmochimica Acta, v. 49, p. 1503–1513.
Ware, J. R., Smith, S. V., and Reaka-Kudla, M. L., 1992, Coral reefs: Sources or sinks of atmospheric CO_2?: Coral reefs, v. 11, p. 127–130.
Winn, C. D., Li, Y. H., Mackenzie, F. T., and Karl, D. M., 1998, Rising surface ocean dissolved inorganic carbon at the Hawaii Ocean Time-series site: Marine Chemistry, v. 60, p. 33–47.
Wollast, R., 1994, The relative importance of bioremineralization and dissolution of $CaCO_3$ in the global carbon cycle, *in* Doumenge, F., Allemand, D., and Toulemont, A., editors, Past and Present Biomineralization Processes: Considerations about the Carbonate Cycle: Musée Océanographique, Monaco, p. 13–34.
Wollast, R., and Mackenzie, F. T., 1989, Global biogeochemical cycles and climate, *in* Berger, A., Schneider, S., and Duplessy, J. C., editors, Climate and Geo-Sciences: Dordrecht, Holland, Kluwer Academic Publishers, p. 453–473.
Wollast, R., Garrels, R. M., and Mackenzie, F. T., 1980, Calcite-seawater reactions in ocean surface waters: American Journal of Science, v. 280, p. 831–848.
Zhong, S., and Mucci, A., 1989, Calcite and aragonite precipitation from seawater solutions of various salinities: Precipitation rates and overgrowth compositions: Chemical Geology, v. 78, p. 283–299.
Zondervan, I., Zeebe, R. E., Rost, B., and Riebesell, U., 2001, Decreasing marine biogenic calcification: A negative feedback on rising atmospheric pCO_2: Global Biogeochemical Cycles, v. 15, p. 507–516.